Mercury capture by native fly ash carbons in coal-fired power plants

James C. Hower [a,*], Constance L. Senior [b], Eric M. Suuberg [c], Robert H. Hurt [c], Jennifer L. Wilcox [d], Edwin S. Olson [e]

[a] University of Kentucky, Center for Applied Energy Research, 2540 Research Park Drive, Lexington, KY 40511, USA
[b] Reaction Engineering International, 77 West 200 South, Suite 210, Salt Lake City, UT 84101, USA
[c] Division of Engineering, Brown University, Providence, RI 02912, USA
[d] Energy Resources Engineering, Stanford University, Stanford, CA 94305, USA
[e] University of North Dakota, Energy & Environmental Research Center, Grand Forks, ND 58201, USA

ARTICLE INFO

ABSTRACT

The control of mercury in the air emissions from coal-fired power plants is an ongoing challenge. The native unburned carbons in fly ash can capture varying amounts of Hg depending upon the temperature and composition of the flue gas at the air pollution control device, with Hg capture increasing with a decrease in temperature; the amount of carbon in the fly ash, with Hg capture increasing with an increase in carbon; and the form of the carbon and the consequent surface area of the carbon, with Hg capture increasing with an increase in surface area. The latter is influenced by the rank of the feed coal, with carbons derived from the combustion of low-rank coals having a greater surface area than carbons from bituminous- and anthracite-rank coals.

The chemistry of the feed coal and the resulting composition of the flue gas enhances Hg capture by fly ash carbons. This is particularly evident in the correlation of feed coal Cl content to Hg oxidation to $HgCl_2$, enhancing Hg capture. Acid gases, including HCl and H_2SO_4 (at small concentrations) and the combination of HC1 and NO_2, in the flue gas can enhance the oxidation of Hg.

In this presentation, we discuss the transport of Hg through the boiler and pollution-control systems, the mechanisms of Hg oxidation, and the parameters controlling Hg capture by coal-derived fly ash carbons.

© 2009 Elsevier Ltd. All rights reserved.

Contents

* Corresponding author. Tel.: +1 859 257 0261.
  E-mail address: hower@caer.uky.edu (J.C. Hower).

1. Introduction

The control of mercury at United States coal-fired power plants has been one of the objectives of the most recent generation of clean air rules from the US Environmental Protection Agency [1,2]. Provisions of the U.S. Environmental Protection Agency's Clean Air Interstate Rule (CAIR) [3] and Clean Air Mercury Rule (CAMR) [4] would have dictated limits the amount of Hg emissions from coal-fired power plants. CAIR would have indirectly cut Hg emissions by calling for increased flue-gas desulfurization of power plants in the eastern United States, while CAMR set strict guidelines for emissions throughout the country. Both would have been enacted by cap-and-trade guidelines. However, in 2008, CAIR and CAMR were vacated by the United States Court of Appeals District of Columbia Circuit [5–7], the latter upheld by the United States Supreme Court [8]. Consequently, in February 2009 the Obama administration's Department of Justice decided to not pursue appeals of the rulings and instead will draft new rules for mercury control. CAIR remains in place until the US EPA issues new guidelines [9]. Some utilities are proceeding with planned construction of flue-gas desulfurization (FGD) units, while others will wait for clarification of the regulations [10].

Engineered solutions, such as the injection of halogenated activated carbon into the flue gas stream [11] have been proposed to capture Hg from the flue gas. Unburned carbon in fly ash will also adsorb varying amounts of the Hg in the flue gas stream. In this paper we discuss the nature of native carbon in fly ash, the controls on Hg capture, and the boiler and ash-collection parameters which influence Hg capture.

2. Mercury in coal

The most fundamental control on the amount of Hg in fly ash is the amount of Hg in the feed coal. The amount of Hg in feed coals varies considerably; for example, for US coals the average Hg content is nearly 0.20 μg/g [2,12], while the delivered coal to US utilities, based on the US Environmental Protection Agency's 1999 Information Collection Request, is about 0.10 μg Hg/g (1999 data) [2]. Differences arise from the overall average being based on a wide range of coals, many not currently mined. The delivered coal average reflects mining practices, coal beneficiation, and utility coal quality specifications, among other variables, all of which can, intentionally or not, serve to reduce Hg in the delivered coal.

If economics and mining conditions permit, Hg in the power plant feed coal can be reduced by not mining Hg-rich lithologies [13–17]. Mercury can be reduced through beneficiation prior to delivery to the power plant [12,18] or through rejection of coarse and/or dense particles by pulverizers [14,17,19,20]. The pulverizer rejects, or "pyrites" as known in the power industry, typically account for less than 1% of the feed coal going to the pulverizers, but can contain >10% of the total Hg in the delivered coal [19].

Hower et al. [20–22] showed that Hg content varied significantly between sites of Pennsylvanian coalbeds in eastern and western Kentucky and Indiana. Mercury in coal has been found to be associated with pyrite and marcasite [23–28]. Mercury has also been found in calcite and chlorite [27]; gold minerals [29,30]; clausthalite and other Pb and Se minerals [31,32];

cinnabar, metacinnabar, and native Hg [33]; getchellite [34]; and kleinite and organic complexes [35]. Yudovich and Ketris [36] provided an extensive review of Hg chemistry in coal, including summaries of the Soviet and Russian literature on the subject. Ding et al. [24], in an electron microprobe study, had proven Hg concentrations in pyrite ranging from 200 to 4700 μg/g. Hower et al. [28], using a scanning electron microprobe, demonstrated that concentrations in marcasite as low as 39 μg Hg/g could be detected. All other Fe-sulfide grains analyzed were within three times the limit of detection; therefore, the values were not significant.

The basic lesson from all of these studies is that Hg is not observed at consistent levels within individual coalbeds, as noted above, but it also does not occur at consistent levels within Fe-sulfides or is it only found in Fe-sulfides. Instead, it is present in other minerals and inorganic combination. Therefore, attempts at simple correlation between Hg and pyritic sulfur are flawed, not only due to the problems in comparing elements present at differences of about five-orders-of-magnitude, such as Fe or S versus Hg, but also due to Hg not always being associated with sulfides.

3. Evolution of unburned carbon in coal-fired power plants

A voluminous literature exists regarding the nature of the char intermediate of coal combustion processes. No attempt will be made here to exhaustively review this literature. Rather, the focus will be on background literature of most relevance to Hg capture by the native char intermediate formed in pulverized-coal-fired boilers, which is the most important anthropogenic source of Hg emissions. Mercury adsorption on coal-derived carbon occurs at temperatures below 300 °C, which correspond to the flue gas cooling zone where carbon combustion has become very slow, so the challenge of describing the carbon sorbent at the point of Hg capture is almost identical to the problem of describing the unburned carbon in ash.

The unburned carbonaceous fraction of coal fly ash has received considerable attention over recent years with respect to its role in boiler efficiency, combustion system operation and the subsequent beneficial use of the ash. Perversely, the same properties that may favor Hg capture (high carbon content, high surface area, and fine particle size distribution) are those that lead to problems in ash utilization, both phenomena being ultimately related to adsorption, as will be seen. It is useful when considering the possible role of unburned carbon in Hg capture, to briefly recount its role in some other important adsorption processes.

Unburned carbon has a significant impact on potential beneficial use of fly ash. If present in large enough amount, this impact is always negative. Generally speaking, utilities will try to run their boilers such that fuel burnout is as high as possible, and hence, unburned carbon in the ash will be as low as possible. There are, however, issues of boiler design, coal selection, and optimization with respect to a variety of emissions requirements that result in an unburned carbon content of around a percent to a few percent by mass in the fly ash from a typical power station. The economic and design considerations that lead to this incomplete combustion generally outweigh the incentives to reduce unburned carbon below a few percent, even if this would make the ash more

attractive for beneficial use. It also should be recalled that a few percent carbon in ash can result even at very high levels of fuel burnout; for example, 99.5% burnout of a 10% ash coal would result in roughly 4% unburned carbon in the ash.

The major beneficial use of coal fly ash in the U.S. is as a pozzolanic additive in concrete [37]. In such use, the presence of unburned carbon can pose a problem associated with adsorption of air entrainment additives (Fig. 1) in the concrete mix [39,40] as well as in certain cases cause problems with color and/or concrete-mix water requirements and behavior. Consequently, commercial processes have been developed for the post-combustor removal of this unburned carbon by burnout in a downstream process (the CBO process of PMI Technologies, LLC) or by electrostatic processes (Separations Technologies, LLC and Tribo Flow Separations, LLC). Tuning the boiler to reduce unburned carbon is indeed possible, but at the expense of an increase in NOx emissions [41]. This is entirely expected, as it is known that air staging for reduction of NOx historically resulted in higher levels of unburned carbon in the ash. Hence, subtle changes in boiler operational parameters can potentially result in significant changes in unburned carbon amounts and properties. Such changes could naturally also impact Hg adsorption capacity of a fly ash. A review of various environmentally driven coal combustion technology changes was prepared by Beer [42].

In certain cases, some of the unburned carbon in a fly ash might actually be soot [40,43], and thus be of a different origin than the usual unburned carbon derived from pyrolytic processes in the solid fuel phase. This ultrafine carbon is believed to be much more active towards air entrainment agents than the usual unburned carbon fraction found in most ashes [40]. This is because very fine, highly dispersed carbon presents a readily available surface for adsorption. Thus, it is also important to have a complete understanding of the nature of unburned carbon for the prediction of adsorptive Hg capture. It is uncommon to find significant amounts of soot material in a well-tuned boiler ash, but if it exists, it could potentially play a significant adsorptive role beyond what its mass fraction might suggest. For a comprehensive review of various aspects of soot in coal combustion, see Fletcher et al. [44].

The unburned carbon in fly ash can also serve as a carrier for other species that are associated with the combustion process itself. This carbon has been cited as a possible site for adsorption of polycyclic aromatic hydrocarbons (PAH) that are produced during combustion, since carbon is a strong sorbent for PAH [45]. The levels of PAH associated with a fly ash are, however, a very strong function of the temperature and excess oxygen used in combustion [46], and the levels from pulverized coal combustion power plants are typically quite low (Wornat et al. [47] found levels of typical 2- to 3-ring PAH in the range of ppb and below). In fact, these inherent PAH levels are usually so low that coal combustion fly ashes might themselves be useful for binding (adsorbing) PAH from other sources (e.g., tar or petroleum spills or releases) found in marine sediments [48]. Fly ash has also been considered as an inexpensive adsorbent for water or soil treatment, such as for adsorption of aromatic acid dyes [49].

Selective catalytic reduction (SCR) or selective non-catalytic reduction (SNCR) processes for control of NOx involve injection of ammonia or urea into fly ash-containing combustion gases, following the main combustion process. If the ammonia is not fully consumed in the process, there exists a problem of "ammonia slip" and some of the unconverted ammonia is adsorbed onto the fly ash. There may also be, in certain instances, ammonia addition to enhance the performance of electrostatic precipitators used to collect the fly ash. Any ammonia adsorbed on fly ash can become an environmental problem when the ammonia is released upon contact of the fly ash with water (see references in Gao et al. [50]).
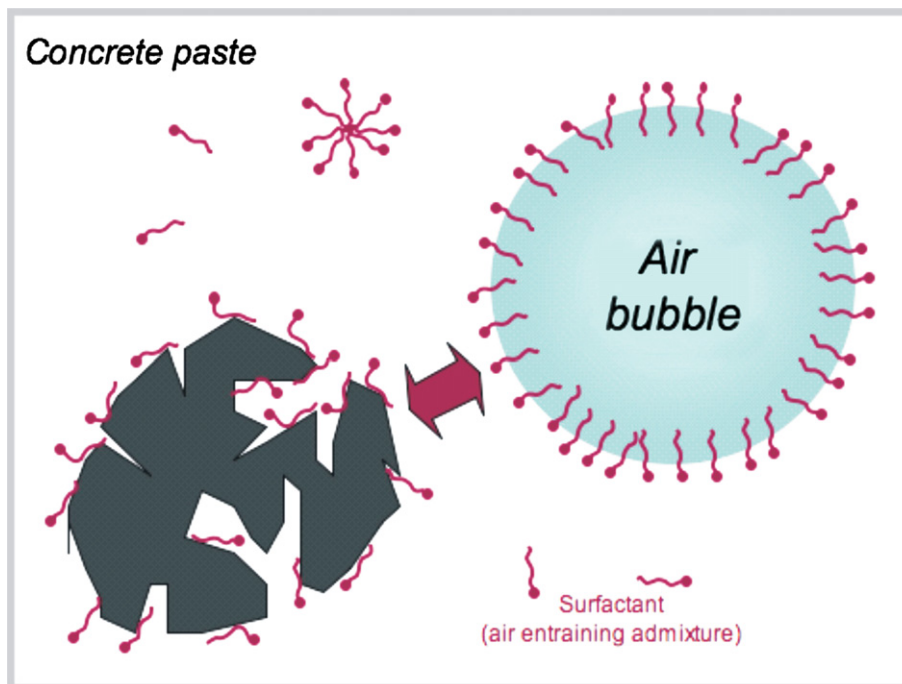

Fig. 1. Sketch of competitive surfactant adsorption that contributes to the deleterious effect of unburned carbon on fly ash utilization when used in concrete as a replacement for Portland cement. The hydrophobic fraction of the carbon surface, not occupied by oxygen-containing functional groups, provides adsorption sites for the hydrophobic portion of the surfactant, or air entraining admixture, and reduces its availability to stabilize air bubbles necessary for freeze-thaw resistance in concrete. The sketch shows a population of amphiphilic molecules (head-tail structure) that make up commercial air entraining admixtures in three different competitive modes of association: (i) at the liquid–gas interface where they serve the intended function of stabilizing air bubbles, (ii) self-associated into micelles in solutions, and (iii) associated with porous unburned carbon (tail adsorption by hydrophobic forces). Adapted from Hachman et al. [38].

SCR processes can influence Hg oxidation (e.g., Lee et al. [51], and discussed elsewhere in this review see Section 5). Ammonia has also been implicated in increasing the release of Hg by leaching of fly ash [52] creating a need to understand the linkage between ammonia sorption and Hg. There have been relatively few fundamental studies of the adsorption process of ammonia on fly ash (e.g., Turner et al. [53]). Pure ammonia has been found to follow more or less standard physisorption behavior on fly-ash carbon surfaces, but it has also been concluded that the high concentrations seen in actual field samples reflects a more complicated chemistry [54].

These studies serve to emphasize that unburned carbon is known to play an important role in adsorption of other species, in addition to Hg, which are present in coal combustion systems. These adsorption processes follow, in many respects, the expected pattern in which the high surface area unburned carbon phase predominates in sorption processes, when compared with the low surface area mineral (inorganic ash) phase. Hence, the remainder of this section will focus on development of available carbon surface during coal char burnout. In this section, the focus is on microscopic surface area, that is, the surfaces contained in submicron and nanometer scale porosity. Section 4 of this review is concerned with carbon morphology on a larger or macroscale, in which petrographic techniques provide information. Both scales are important – the microscale for establishing the overall extent of available surface, and the macroscale for determining how readily available this surface is for species present at the nominal geometric surface of the ash (or unburned carbon) particles.

3.1. Evolution and modeling of coal char structure during burnout

There have been numerous studies that have examined the nature and amount of unburned carbon from pulverized coal combustion systems [19,43,55–84]. This selection of papers is by no means complete, and primarily more recent studies, and those with a tie to Hg capture, have been emphasized in this review. There are some general conclusions that may be drawn from the above studies.

Utility boilers operate at quite high carbon conversions, most often well over 99% [85]. Typical unburned carbon in fly ash ranges from around one percent by mass to a few tens of percent, with well-tuned boilers typically giving ashes with unburned carbon well below 10%.

Unburned carbon levels in ash depend in a complicated way on boiler type, operation (e.g., pulverizer performance, air staging), and fuel selection. Power stations that use a range of coals, often including internationally traded coals, have found systematic fuel-to-fuel differences, which are believed to result from differences in grinding and classifying behavior, char yield, char reactivity, and char morphology as affected by coal rank, type, and mineralogy.

There are a variety of different carbon types that may be found in the ash. The generally predominant form is char derived from pyrolysis of the coal, which leads to discreet, carbon-rich particles clearly visible in ash under the optical microscope (Fig. 2). Soot also forms in the fuel-rich, near-burner zones, but, due to its ultrafine size, burns out readily in the oxygen-containing post-flame zones unless it fails to contact oxygen by burner imbalance or poor mixing of secondary, tertiary, or overfire air [40,43] and thus soot, the nano scale carbon form, is not commonly a major contributor though may play an adsorptive role in some special cases [75].

Related to the preceding point, there is always a distribution of unburned carbon particle sizes in the ash [67] and a distribution of unburned carbon in different size fractions of the ash [55,78]. It is quite common to find a high fraction of unburned carbon mass in relatively large particles with a high carbon content [55,67,78],
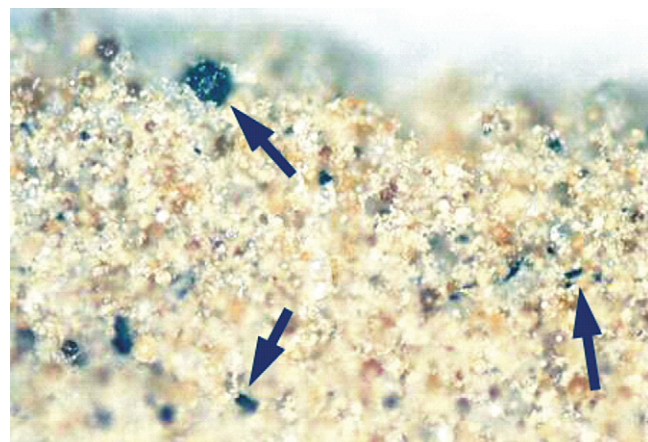

Fig. 2. Optical micrograph of fly ash sample from full-scale utility boiler. Arrows show discreet carbon-rich particles that make up the major fraction of unburned carbon in most samples. Adapted from Kulaots et al. [67].

though this is not necessarily always the case. Fig. 3 shows examples of size distributions for the total fly ash, while Fig. 4 shows the distributions for the carbon component alone. The unburned carbon is typically significantly coarser than the mineral component of the ash (Fig. 3) due to differences in the natural grain sizes of the two components in the feed coal. In this dataset (Fig. 4), the carbon size distribution is also coal rank dependent, with low-rank coals showing a larger percentage of the total carbon in the largest two size categories (>180 um). A number of factors may contribute to this trend, but it is likely that the dominant effect is the higher overall burnout for low-rank coals – when a polydisperse population of char particles burns in a diffusion influenced regime, the size distribution becomes *coarser* as small particles burnout leaving
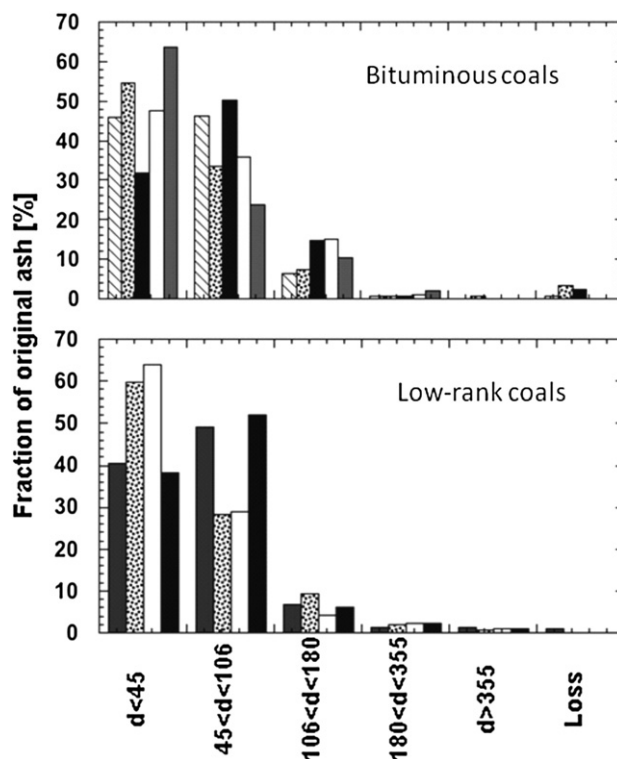

Fig. 3. Particle size distribution (wt-%) of whole fly ash samples from full-scale utility boilers for nine parent coals. Different bar patterns represent different parent coals in each panel. Adapted from Kulaots et al. [67].
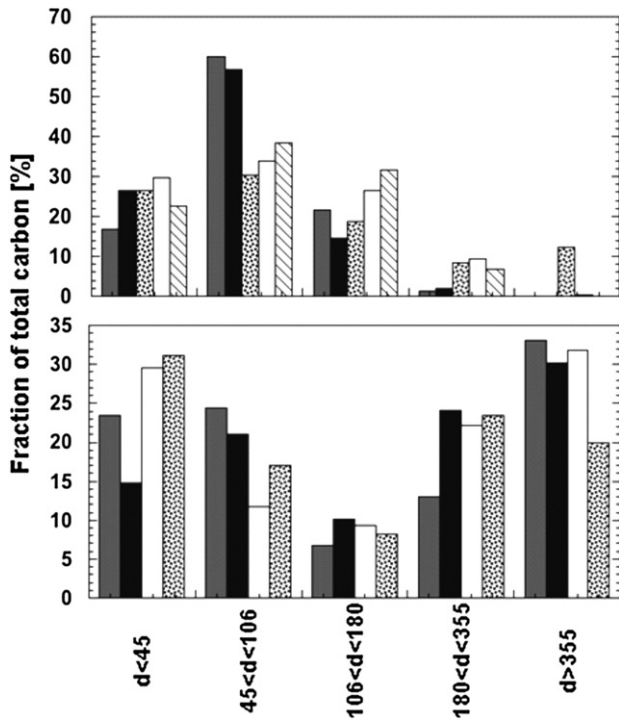
Fig. 4. Particle size distribution (wt-%) of the unburned carbon fraction of fly ash sampled from full-scale utility boilers for nine different parent coals. Different bar patterns represent different ash/parent-coal samples from the field. Adapted from Kulaots et al. [67].

larger particles increasingly concentrated in the unburned carbon fraction of ash.

- There is general agreement that carbon surface area does play some role in adsorption of various species present in the combustion environment. Fig. 5 shows that the nitrogen BET surface areas of the carbon fractions themselves are typically 20–70 m^2/g-carbon for unburned carbon derived from
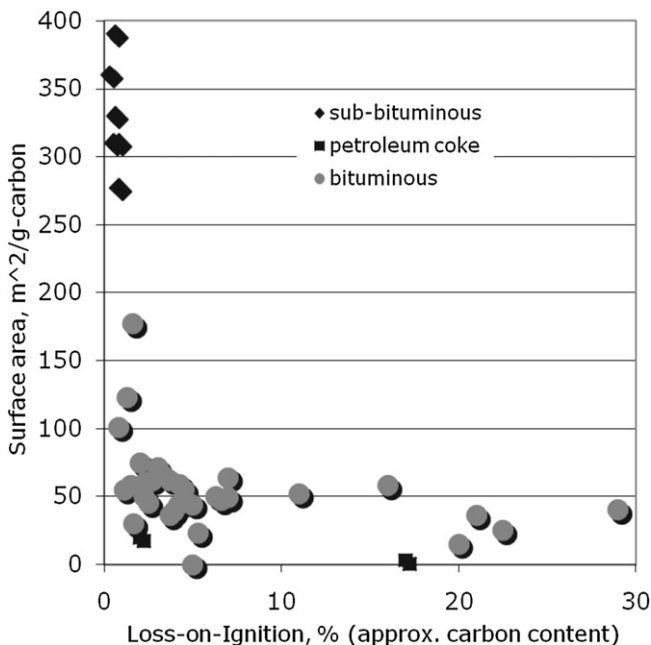

Fig. 5. Surface areas per unit mass of carbon in a collection of fly ash samples from full-scale utility boilers. Adapted from Gao et al. [58].

bituminous coals and 300–400 m^2/g-carbon for unburned carbon derived from lower-rank (non-softening) coals [58]. The possible range of surface areas is strongly imprinted by the choice of coal, but there is an influence of combustion environment. The implication is that final burnout is taking place under partial mass transfer limited (Zone II) conditions [66]. Fig. 6 provides evidence that the full-scale combustion process occurs in a regime influenced by oxygen diffusion. The surface area of unburned carbon in ash can be greatly increased (the carbon can be "activated") by subsequent reaction with oxygen at low temperatures.

- The total sorptive area of a fly ash will be determined mainly by its carbon content, since the mineral portion normally has very low surface area (<1 m^2/g-inorganic ash [58]).
- Within the coal-derived unburned carbons there exist a wide range of different morphologies whose presence and structures depend upon the nature of the starting coal and the combustion conditions.

The key features of interest with respect to the potential of unburned carbon to contribute to Hg capture are its amount, size distribution, surface area, and surface chemistry, all of which vary through the combustor as the char burns out. It has been well established that the amount of carbon in fly ash generally plays some role in determining its capacity to sorb Hg [19,70–72,75,77,79,86,87], since carbon is the main sorptive species in the ash. There are clearly issues of morphology and surface chemistry that are known to play important roles as well [64,75,78–80]. In this section on the combustion process, we focus on the amount of carbon that is left in a fly ash, its size distribution, and its surface area. Other important factors such as char surface chemistry, the role of heteroatomic species (especially the halogens), the nature of the contacting of the ash, and Hg (especially temperatures and residence times) are covered in other sections of this review.

The overall outline of the coal combustion process is generally understood. The reader can refer to many different summaries of the process, such as those by Essenhigh [88] or Smoot [89]. As coal is first heated in the boiler, it devolatilizes, giving off tars and gases. Depending upon particle size and coal composition, as well as on the mixing characteristics of the boiler, combustion may initially take place in the vapor phase in a volatile-rich phase, or the particle might ignite on its surface [88]. Here, there will be no further consideration of volatiles combustion, but rather an emphasis on
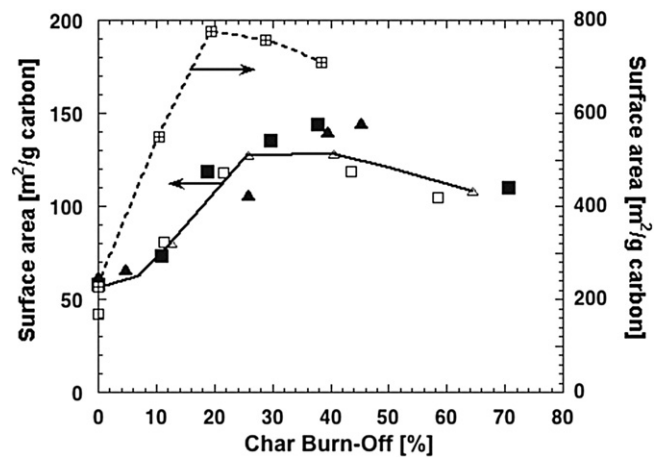

Fig. 6. Development of surface area in full-scale unburned carbon samples through post-capture air oxidation at low-temperature in the laboratory. Different symbols represent different field ash samples, which originated from different parent coals and operating conditions. Adapted from Kulaots et al. [66].

factors determining the final char structure. It is useful to note, however, that depending upon the details of the combustion system, soot formation is strongly tied to volatiles chemistry. If the burnout of the soot is incomplete, there can be an influence of volatiles processes on unburned carbon in fly ash.

During the pyrolytic phase in the bituminous coals, the organic matter will typically soften, whereas in the case of low-rank coals, the organic matter will generally behave in a thermosetting (non-softening) manner. The fluidity of the pyrolyzing organic matter largely determines the observed morphological characteristics of the char, and different macerals within the same coal will behave differently (some may soften, others not). If the particles soften during pyrolysis, then a fluid with low amounts of "free volume" forms, and upon resolidification, there is no mechanism for large amounts of porosity to be re-created. Within a single coal, the unburned carbons from inertinite macerals have been shown in one case to have the lowest density and surface area, followed by those that are isotropic and anisotropic [69].

The actual burnout of the char will follow processes dictated by both the reactivity of the char as well as the mass transfer characteristics in the boiler. Porous solid–gas reactions are often characterized by three reaction regimes: kinetic control (sometimes called Zone I), pore diffusion control (Zone II), and film diffusion control (Zone III), with the shorthand zone nomenclature adopted from the work of Walker et al. [90]. It was once commonly assumed that the temperatures of combustion, and thus rates, are sufficiently high in pulverized coal combustors that the combustion mostly takes place under Zone III conditions. This view is, however, not consistent with observations. The more generally accepted view is now that pulverized coal chars burn under Zone II conditions, at least in later, lower-temperature regions of a boiler where the final char burnout is occurring, and in this regime the carbon reactivity does appear to impact observed results [66,85,91].

Added to these time-dependent processes are significant three-dimensional spatial variations in full-scale boilers that make the modeling of coal combustion processes in the field exceptionally complicated. The chemistry of the pyrolytic process already involves large numbers of distinct chemical species, and the combustion processes add many more (not all of which are even firmly established). Onto this must be added the complexities of heat transfer and fluid flow, and the physical processes in the solid phases (including both the organic phase as well as the ash phase). Summaries of some of the relevant combined computational fluid dynamics (CFD)-combustion models have been published [89,92,93]. There remain important questions regarding the ability of the CFD-based models to correctly predict unburned carbon values at the level of accuracy that might be required for predicting Hg capture [94,95].

A different approach to modeling the char burnout process is that embodied in the so-called CBK (Char Burnout Kinetics) model [96]. In this model, the focus is on the problem of carbon burnout, and the aim was particularly the prediction of the late stages of carbon burnout. The CBK model is not intended to be a complete combustor model, as are the others alluded to above, but rather, to be a stand-alone computation of char burnout, provided that a particular system can somehow be characterized with respect to relevant temperature-time characteristics (something that is inherent in the CFD models). The CBK model includes a statistical kinetics description of char combustion, as well as the process of annealing. It also includes inhibition of the kinetics by an ash layer. It has been implemented in another code designed to predict unburned carbon levels in fuel switching scenarios, again without explicit reference to fluid flow or transport processes in a full-scale boiler [97]. The model has also been extended by Stephenson [98], and in modified form by Cloke et al. [99] and Wu et al. [100]. It has

also been grafted onto a CFD approach, in a two-step calculation [94,101,102]. Another integration into a CFD code has been described [103], but comparison of predictions to actual full-scale combustor results were not available. A different, detailed particle-level combustion model has recently been presented, that seeks to predict the development of surface area and particle morphology under both Zone I and Zone II conditions [104]. Again, this latter model seeks to predict behavior, assuming information is separately available on the particle environment.

There is a significant challenge for any effort at modeling coal combustion with an eye towards predicting the adsorptive properties of unburned carbon. First, the accurate prediction of unburned carbon levels, at the desired level of accuracy, is beyond what can be expected from any of the CFD-based computation models at the present time. Factors of two in unburned carbon predictions might be hardly noticed in models aimed at capturing the main features of heat transfer and gas-phase processes, but will make a large difference in determining Hg-sorption capacity. Beyond this, not even the more detailed burnout models attempt to get into the prediction of porosity or into the details of fragmentation (prediction of unburned carbon particle size distributions). Both features are known to be important in adsorption processes. Prediction of porosity development during combustion and gasification involves a significant effort in and of itself [105,106]. This effort is in addition to that needed to describe the formation of bubble and void structures in softening coals [107,108], or the fragmentation of particles during combustion [84,109].

4. Fly-ash carbon morphology

The classification of fly ash carbons has gone through a number of iterations through the years [60–62,110–115]. Based on those discussions, and on the philosophy behind coke petrography [116], Hower et al. [117] developed a system suitable for the bituminous-coal-derived fly ashes of the eastern US. Unlike the morphology-based descriptions of Bailey et al. [62], their system relied more on the optical properties of the carbons, dividing the neoformed vitrinite- and semi-inertinite-derived carbons into isotropic and anisotropic cokes or chars (Fig. 7). Inertinite-derived carbons pass largely intact through the boiler (Fig. 8), although some alteration can be detected (Fig. 9). As noted by Hower et al. [118], "although fly ash inertinite is likely derived from inertinite in the coal, it cannot be said that isotropic and anisotropic chars are derived strictly from vitrinite." Relatively unburned, albeit slightly devolatilized, coal is

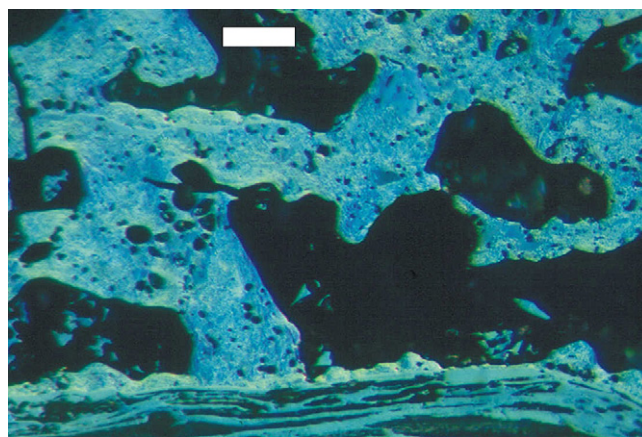
Fig. 7. Inertinite (bottom) with anisotropic coke from combustion of high volatile A bituminous central Eastern Kentucky coal. Reflected-light, oil-immersion optics with crossed nicols, wavelength plate, (scale = 270 microns along long edge).
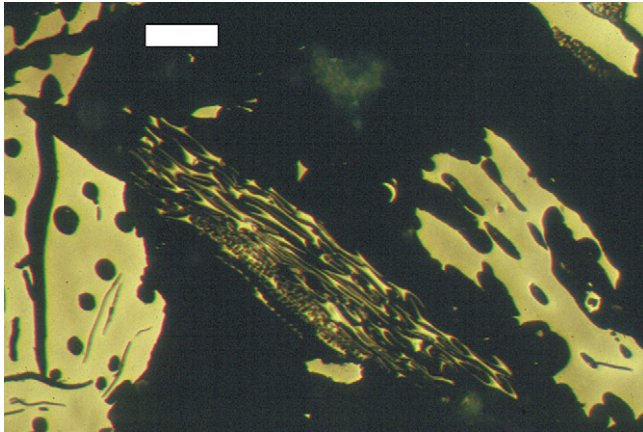
Fig. 8. Variety of inertinite forms from power plant burning high volatile A bituminous Central Appalachian coal. Reflected-light, oil-immersion optics, (scale = 25 microns).
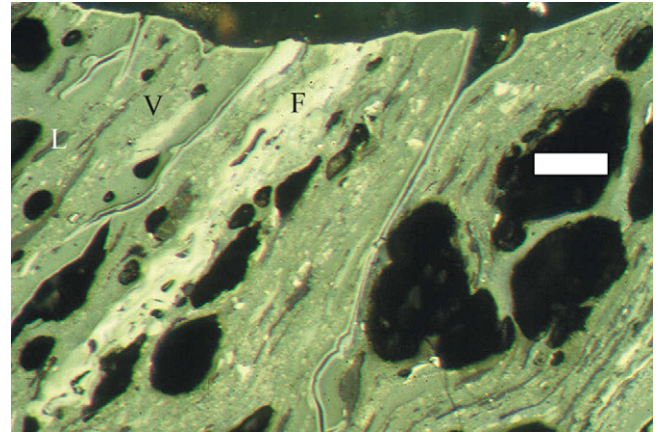

Fig. 10. Partially burned coal with devolatilization features: remnant liptinites (L), vitrinite (V), and fusinite (F); and oxidation rims along particle edges and along fractures. Reflected-light, oil-immersion optics, (scale = 25 microns).

rare (Fig. 10). Hower and Mastalerz [119] developed a system which combined aspects of the Hower et al. [117] optical-properties system and the morphology-based system of Bailey et al. [62] and the International Committee for Coal and Organic Petrology [120]. Hower et al. [118] later expanded the definitions to include coal of lower and higher rank than the bituminous coals of the original system.

Coal rank is an important factor in determining the type of carbon in fly ash. Vitrinite/huminite (nomenclature for vitrinite/ huminite and inertinite group macerals can be found at ICCP [121,122] and Sykorova et al. [123]) from low-rank coals generally does not form the isotropic and anisotropic carbons seen in bituminous-coal-derived fly ash. Upon heating, low-rank coals do not undergo thermoplastic transitions. Rather, the chars derived from low-rank coals are dominated by forms that are devolatilized, but without the devolatilization vesicles of higher-rank coals (Fig. 11). Bituminous coals will generally swell and undergo thermoplastic transitions upon heating to 300–400 °C [116]. In the boiler, such plasticity leads to neoformed (generally) vitrinite-derived structures (Fig. 4.1), and to carbon cenospheres. In coals of any rank, coal included within rock may be carbonized, but it will generally not be combusted nor exposed to the flue gas, therefore, the carbon would not be accessible for Hg capture (Fig. 12).

Coals of semi-anthracite rank and higher generally do not display thermoplastic properties. Vesiculated chars have been

observed in anthracite-derived fly ash carbons and porous chars have been noted in meta-anthracite-derived chars [70,71,118]. Both isotropic and anisotropic chars have been seen in fly ashes from high-rank coals (Fig. 13).

Using high-resolution transmission electron microscopy, scanning transmission electron microscopy, and electron energy-loss spectroscopy (HRTEM-STEM-EELS), a fullerene-like carbon form has been found in emissions from power plants as well as in the form of a deposit on glassy particles in bituminous-coal-derived fly ash [43,74,78,124–127]. To date, low- and high-rank-coal-derived fly ashes have not been investigated for the presence of this carbon form. As seen in Fig. 14 (Fig. 3 from Hower et al. [74]), the carbons can form bridges, presumed to be rather fragile, between the glassy Si-Al spheres dominating this and most fly ashes. The small, few-nm, dark spots in Fig. 14 are metal grains. The chemistry of these grains will be discussed in Section 6.

5. Hg chemistry in boilers and APCDs

The principal Hg input stream to a coal-fired boiler is the coal. The form of Hg in the coal is either mineral-bound (often in the sulfide phase) or organically associated, as discussed in Section 2. In either case, in the high temperature of the flame in a coal-fired boiler, all the Hg is expected to be in the vapor phase [128,129]. Mercury is expected to be in the gaseous elemental form in the
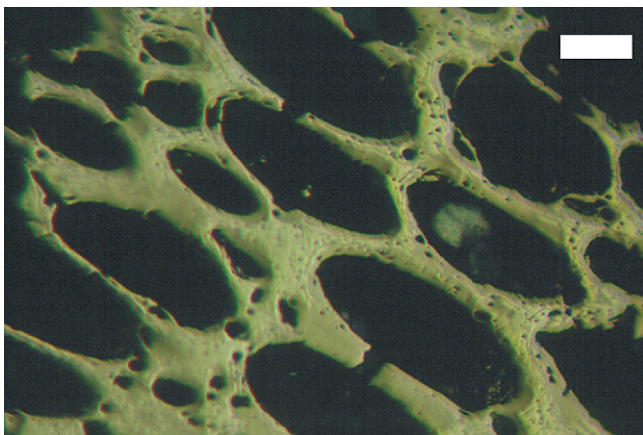

Fig. 9. Inertinite from a power plant burning high volatile A bituminous central Eastern Kentucky coal. Note incipient breakdown of inertinite cell walls. Reflected-light, oil-immersion optics, (scale = 25 microns).
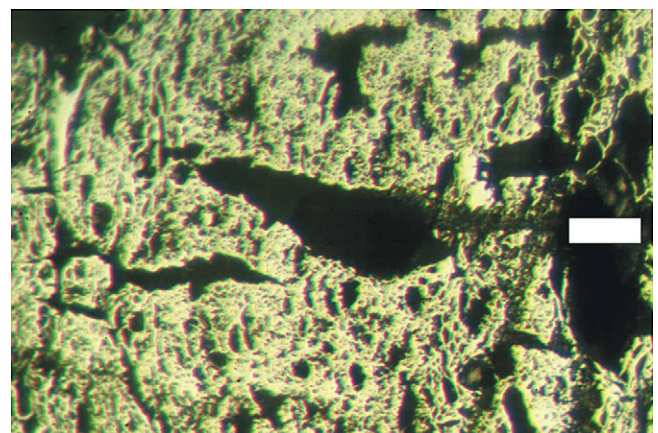

Fig. 11. Isotropic char from the combustion of subbituminous western US coal. Reflected-light, oil-immersion optics, (scale = 25 microns).
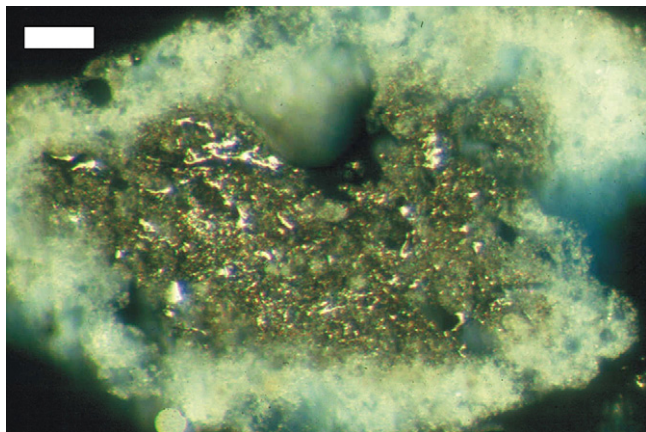
Fig. 12. Vitrified outer boundary of particle. The interior has been thermally altered; note high reflectance carbons. From Tennessee power plant burning medium-sulfur, high volatile A bituminous Central Appalachian coal. Reflected-light, oil-immersion optics, (scale = 25 microns).
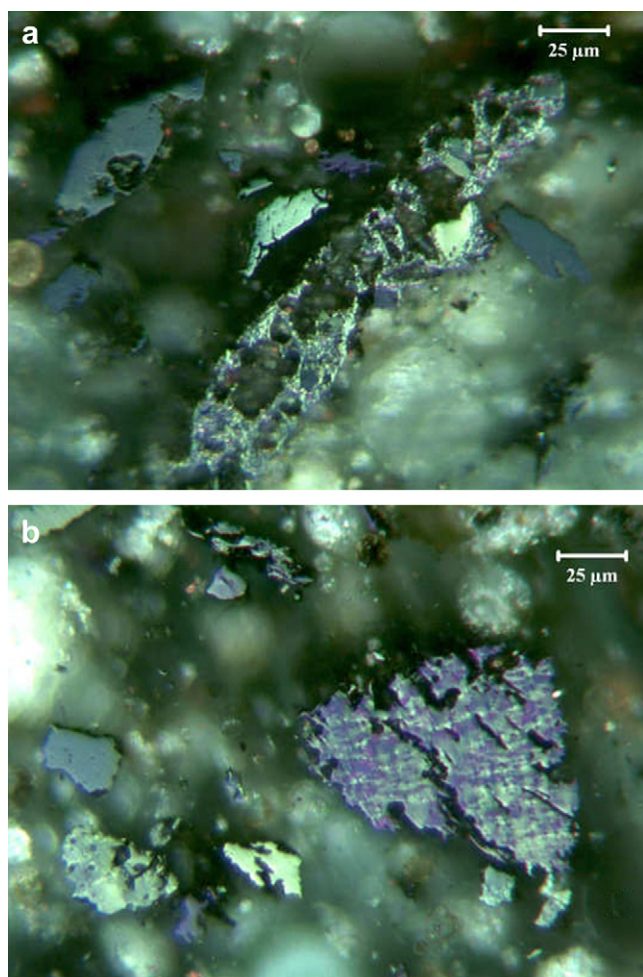

Fig. 13. Fly ashes from Portuguese power plant burning anthracite. Sample courtesy of Bruno Valentim, University of Porto. Scale bar is 25 microns on both images. Reflected-light, oil-immersion optics with crossed nicols, wavelength plate. a/Anisotropic coke (across diagonal) and other anthracite-derived carbons. b/Vitrinite-derived anisotropic carbon (right center), perhaps without significant alteration from feed coal, and other anthracite-derived carbons.

flame, according to equilibrium calculations [128,130]. In a coal-fired boiler, the flue gases cool from high temperature (~1600 K) to the temperature at the inlet to the air pollution control devices (APCDs) (400–450 K) with a cooling rate of ca. 300 K/s (Table 1; Fig. 15) [130]. Given the elements that are typically present in coal and air, thermodynamic equilibrium predicts that Hg will be gaseous HgCk at the temperature of the inlet to the APCD for the range of chlorine observed in US coals, which is 10–4000 μg/g [128,103]. Transformation of elemental to oxidized Hg involves both gas-phase (homogeneous) reactions [131–137] reactions [138–142]. The homogeneous oxidation of elemental Hg to HgCk is kinetically limited in coal-fired boilers [130]. Heterogeneous oxidation is more complicated, but the observation that the percentage of oxidized Hg at the inlet to APCDs was limited by coal chlorine content [144], suggests kinetic limitations on both homogeneous and heterogeneous oxidation. Therefore, some fraction of the Hg is oxidized at the inlet to the APCDs.

As a result of chemical transformations in the flue gas, Hg enters the APCDs as a mixture of species. The methods available to measure Hg in coal flue gas can distinguish among gaseous elemental, gaseous oxidized, and particulate-bound Hg. Each of these different forms of Hg behaves differently in APCDs. The extent of Hg oxidation or conversion to particulate-bound Hg depends on the flue gas composition, the amount and properties of fly ash, and the flue gas quench rate. Theoretical models have been developed to predict mercury speciation in coal-fired power plants [136,139,142] with moderate success.

A survey of the types of APCDs on coal-fired electric utility boilers in the US was carried out using NETL's 2007 Coal Power Plant Database, which includes data from the DOE EIA-767 database [143]. Table 1 summarizes the major types of APCDs on coal-fired utility boilers in terms of total boiler capacity; the data have been subcategorized by type of APCD and by the rank of coal burned.

The most common particulate control device (PCD) in U.S. coal-fired utility power stations is an electrostatic precipitator (ESP), used with or without flue-gas desulphurization (FGD) for SO$_2$ control. Most ESPs are "cold-side" or C-ESP, that is, they operate at temperatures in the range of 400–500 K. Subbituminous- and lignite-fired plants have predominantly cold-side ESPs without any desulphurization equipment: 65% and 80% have C-ESPs, respectively. A small number of ESPs are "hot-side" or H-ESP, and operate at 620–670 K. In an ESP, there are a number of electric fields arranged in series with respect to the gas flow. Particles are collected on charged plates in each field. Periodically the plates are rapped and the accumulated ash layer falls into a hopper below. Typically each field of an ESP has a hopper associated with it. Ash collection takes place serially, with most of the ash being collected in the first field and lower amounts in subsequent fields.

A fabric filter (FF) is the other common PCD, which may be used alone or with a spray dry adsorber (SDA), the latter to remove SO$_2$. Fabric filter collectors have a series of compartments, each containing a number of bags on which the ash is collected. Each compartment has a hopper where the ash is collected upon cleaning the bags. Bags are cleaned by mechanical agitation or pulsing with air. Compartments are cleaned when the pressure drop across the bags reaches a certain level. In an ESP, there is a distinctive pattern of collection from one ESP field to the next, as discussed above, which means that the size and amount of material collected varies among the hoppers of different fields. However, in a fabric filter, ash collection does not follow such a distinctive patter as in an ESP.

Ten percent of the low-rank-fired plants have fabric filters and 10% of the subbituminous-fired plants have hot-side ESPs. Many
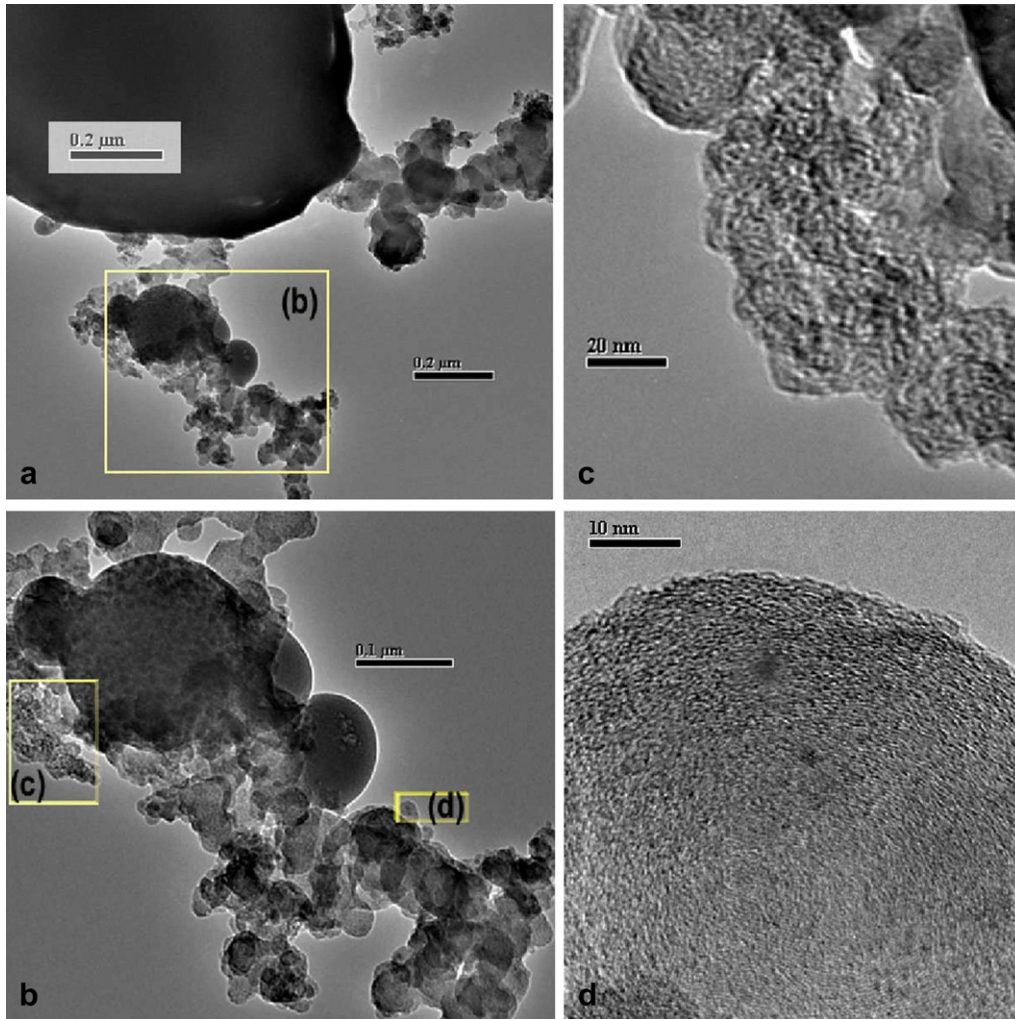
Fig. 14. High-resolution transmission electron microscope (HRTEM) images of C-rich nano-clusters. Large dark round bodies in 14a and 14b and at extreme upper right of 14c are Si-Al glass fly ash particles. Carbon surrounds Si-Al particles and acts as a bridge between Si-Al grains. Few-nm dark spots within carbon in 14d are metal grains, (scale: a – 0.2 microns; b – 0.1 micron; c – 20 nm; d – 10 nm). (after Hower et al. [74])

boilers have a selective catalytic reduction (SCR) unit for removal of nitrogen oxides (NOx).

As part of EPA's Information Collection Request (ICR), data were collected on Hg speciation and Hg removal across air pollution control devices at 83 full-scale power plants. For power plants in the EPA study, the percentage of Hg that was oxidized at the inlet to the PCD increased with increasing coal chlorine content [144]. The amount of elemental Hg at the inlet to cold-side ESPs was less than 20% as long as the coal Cl content was greater than about 500 $\mu g/g$. Bituminous coals from the U.S. typically would have greater than 500 $\mu g/g$ Cl [2]. Thus, bituminous coal-fired power plants are expected to have higher amounts of oxidized Hg in the flue gas.

The average Hg removal across the wet FGDs in this dataset was well over 50% for bituminous coals but only about 30% for subbituminous coals [144,145]. The amount of Hg removed across a wet FGD depends largely on how much oxidized Hg is present at the scrubber inlet [146]. SCR systems have been observed to oxidize Hg in coal-fired power plants [147–149] and the range of Hg oxidation observed in plants firing bituminous coals was 30–98%. Limited data from plants burning subbituminous coal suggests much lower amounts of Hg oxidation across SCRs in these plants. Subbituminous coals and lignites have lower Cl than bituminous coals [2]. Modeling of Hg oxidation across SCRs (Senior, 2005) has

demonstrated that coal Cl content is one of the key factors affecting Hg oxidation across SCRs.

The combination of an SCR and a wet FGD scrubber can remove 90% or more of the Hg (from input to stack), if there is sufficient oxidized Hg at the scrubber inlet. Withum [150] measured Hg removal on eight bituminous coal-fired boilers with SCR and FGD; average Hg removal (coal to stack) on these boilers varied from 65 to 97%.

A review of some of the data collected from full-scale systems showed that Hg removal across ESPs in pulverized-coal-fired boilers burning bituminous coals appeared to be related to the LOI

Table 1
Distribution of air pollution control devices on coal-fired power plants in the U.S by total capacity in MW.

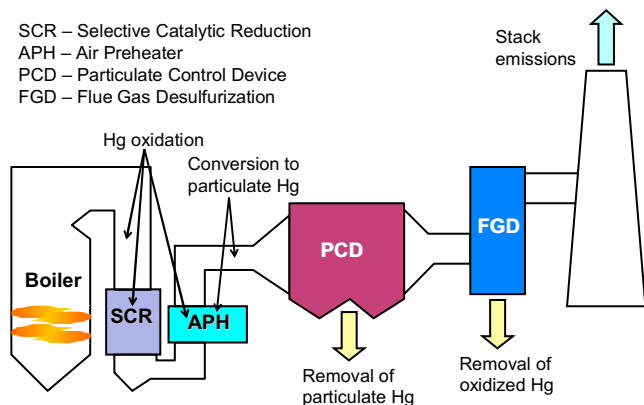|	Bituminous	Subbituminous	Lignite
FGD-SCR (all PCDs)	68,204	6518	0
SDA (all PCDs)	5552	8711	1320
C-ESP (except FGD-SCR)	81,289	88,357	10,714
FF	9942	12,712	1376
H-ESP	16,615	13,204	0
Other	535	7534	50
Total	182,138	137,037	13,460

Fig. 15. Behavior of mercury in common air pollution control devices in coal-fired power plant.

Fig. 16. Size distribution of fly ash collected by economizer, mechanical (cyclone), and electrostatic precipitators at a Kentucky power plant burning southeastern Kentucky high volatile A bituminous coal.

or unburned carbon in the fly ash [77]. Sulfur in the flue gas has been shown to negatively affect capture of Hg by carbon, and the effect is most pronounced where both LOI and coal Cl are high, and is consistent with the notion that sulfur fills reactive sites on fly-ash carbon [140]. Data reported by the Canadian Electricity Association [151] for two units equipped with cold-side ESPs showed that Hg capture across the C-ESP decreased as coal sulfur increased.

Sjostrom et al. [152] estimated the LOI of the fly ash from ICR plants equipped with fabric filters. Good Hg removal was observed across fabric filters in the ICR database for boilers burning bituminous and subbituminous coals, an average removal of 70 and 84%, respectively. Little removal was observed across fabric filters in lignite-fired plants. Sjostrom et al. [152] did not observe a correlation between Hg removal across fabric filter and LOI, coal Cl, or temperature.

In summary, APCDs collect Hg via two pathways: removal of particulate-bound Hg in particulate control devices and removal of gaseous oxidized Hg in flue-gas desulphurization (FGD) scrubbers or spray dryer absorbers (SDAs). The behavior of Hg in air pollution control devices is summarized in Fig. 5-1.

6. Distribution of mercury in fly ash collection systems

The distribution of trace elements within fly ash collection systems is, first, dependent upon the concentration of elements in the feed coal [16,17,130,153–168]. Following combustion, the partitioning of volatile trace elements, such as Pb, As, and Zn, within the electrostatic precipitator (ESP) or baghouse or fabric filter (FF) array is a function of the temperature of the flue gas at the collection point and the ESP or FF row [14,19,114,115,153,169–175]. Specifically, trace element concentration will generally increase towards the back rows of the collection system, coincident with a decrease in the flue-gas temperature and a decrease in the particle size of the fly ash and a concomitant increase in the fly ash surface area. The latter is a consequence of the first rows of the pollution-control system scalping off the coarser fly ash particles, leaving the finest particles in the final rows (Fig. 16).

Capture of Hg by fly ash varies from the behavior of other volatile elements [16,69,72,75,130,159,160,176–184]. Li et al. [79], however, in a study of seven different bituminous coals burned in the same 100-MW boiler studied by Sakulpitakphon et al. [185], could not discern a relationship between the amount of feed-coal Hg and the fly ash Hg. They [79] did not mention whether the analyzed coal was the delivered coal or the pulverized coal. Aside from the variations in the amount of Hg in the boiler feed coal (Section 2), Hg concentrations in fly ash have proven to be largely a function of the (a) amount of
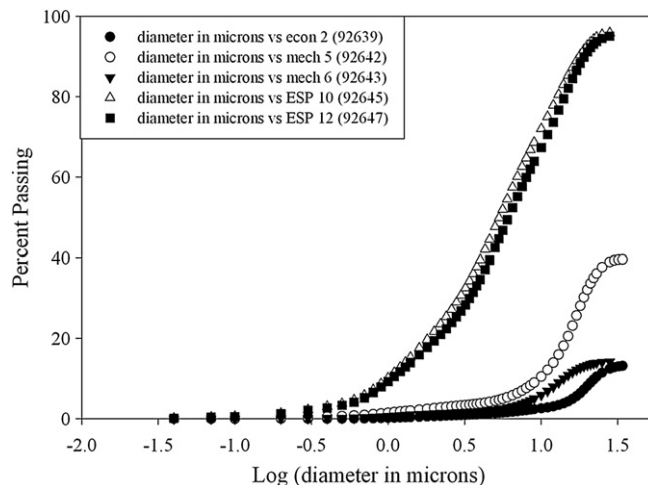
carbon, (b) the flue-gas temperature at the point of collection, (c) the composition of the flue gas, and (d) the type of fly ash carbon, including variations dependent upon the rank of the feed coal. Each of these variables will be discussed below.

6.1. Variation in mercury capture by amount of fly ash carbon

Within a single field of an ESP or FF (that is, within the ash collected in the row of the hoppers corresponding to that field), Hg can be correlated with the amount of carbon in the fly ash [14,16,19,174,185,186]. Hower et al. [174] analyzed Hg from wet-screened[1] fly ash collected in consecutive months from the same ESP row at a Kentucky power plant. They found that Hg was highly correlated to fly-ash carbon (Fig. 17), with the important caveat that both the flue-gas temperature at the collection point and the feed-coal source were similar between the two collection times. Hower et al. [184] extended the correlation to the mechanical separation prior to the FF array and to the FF hoppers at a western Kentucky power plant. Among all of the variables investigated by Li et al. [79], fly-ash carbon was one of the stronger correlations to Hg capture. They only obtained one ESP fly ash sample for each of the feed-coal burns studied; therefore, their investigation could not discern carbon versus Hg trends within or between ESP rows for each of the coals.

The conversion of boilers to low-NOx combustion systems through the 1990s resulted in a general increase in carbon in the post-NOx-conversion fly ash [189], although this was not always the case [190]. The fly ashes obtained from ESPs from several of the conversions were later analyzed for Hg and showed generally good intra-row Hg versus fly-ash carbon correlations, including the near coincidence at zero of the extrapolated Hg and fly-ash carbon (Fig. 18).

6.2. Variation in mercury capture by flue-gas temperature

Many of the studies cited in Section 6.1 also addressed the variation of Hg capture by flue-gas temperature at the collection point. In the studies discussed, while the temperature is not exactly

---

[1] Researchers at the University of Kentucky Center for Applied Energy Research have employed wet screening to separate fly ash into size fractions. While there may be some loss of trace elements to the water, the alternative, dry screening, does not make an accurate separation at fine sizes [187,188].
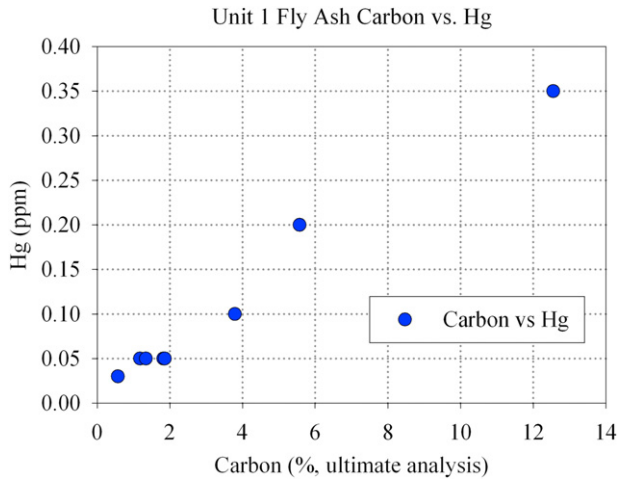
Fig. 17. Fly-ash carbon versus mercury content in the fly ash in wet-screened fly ashes from two collection times of the same row of a Kentucky power plant burning a high volatile bituminous Illinois Basin coal blend (after Hower et al. [174]).

known, it is known that the flue-gas temperature does decrease with increased distance from the boiler.

The study of an Appalachian-low-S-coal-fired power plant with a three-row mechanical/five-row baghouse (FF) ash collection system [184], mentioned above, is notable for the difference in Hg levels between the two parts of the system (Fig. 19). The mechanically-separated (cyclone separation) fly ash has higher carbon content than the FF fly ash but, owing to the higher flue-gas temperature, the Hg content of the mechanical fly ash is significantly lower than the FF fly ash.

Multi-year studies at a power plant with a five-row-ESP-ash-collection system, also burning central Appalachian coal, demonstrated a clearer relationship between Hg versus C within ESP rows, as well as a clear relationship with ESP row as a proxy for flue-gas temperature. With the exception of two hoppers on the fourth ESP row, the same hoppers were sampled in both 2004 and 2007. The fifth row hoppers were empty on both sampling dates. Fig. 20 (based on unpublished data, University of Kentucky Center for Applied Energy Research) demonstrates: (1) a general increase in Hg in the ash from the later fields of the ESP, implying a lower flue-gas temperature; and (2), for both years, an increase in Hg with fly-ash carbon (carbon based on ultimate analysis of fly ash). The differences in Hg in rows 3 and 4 for 2007 versus 2004 is a function of the amount of fly ash carbon, perhaps among other unquantified parameters, and not to the amount of Hg in the feed coal, 0.09 µg/g for both years.

In separate studies at a 200-MW utility boiler with (initially) a two-row mechanical and three-row-ESP-ash-collection system, Mardon and Hower [14] and Hower et al. [186] demonstrated the complexity of the Hg-carbon relationships for up to three rows of the ESP for five different collections from 2001 to 2007 (Fig. 21). For the row-by-row collections, as best as possible, collections from each row followed a straight path through the ESP array. Two important caveats must be considered in examining this data. First, the coal source, while always from the central Appalachians, usually southeastern Kentucky, did change throughout the period examined as the company purchased some of their coal on the spot market. Second, for collections after 2002, the utility modified the collection system through the bypassing of the mechanical hoppers. For the 2004 and 2007 collections, all of the post-economizer fly ash passed directly to the ESP's. In contrast to many other plants examined, carbon is relatively more abundant in the later rows of the ESP than in the first row [170,191]. Fig. 22 illustrates the
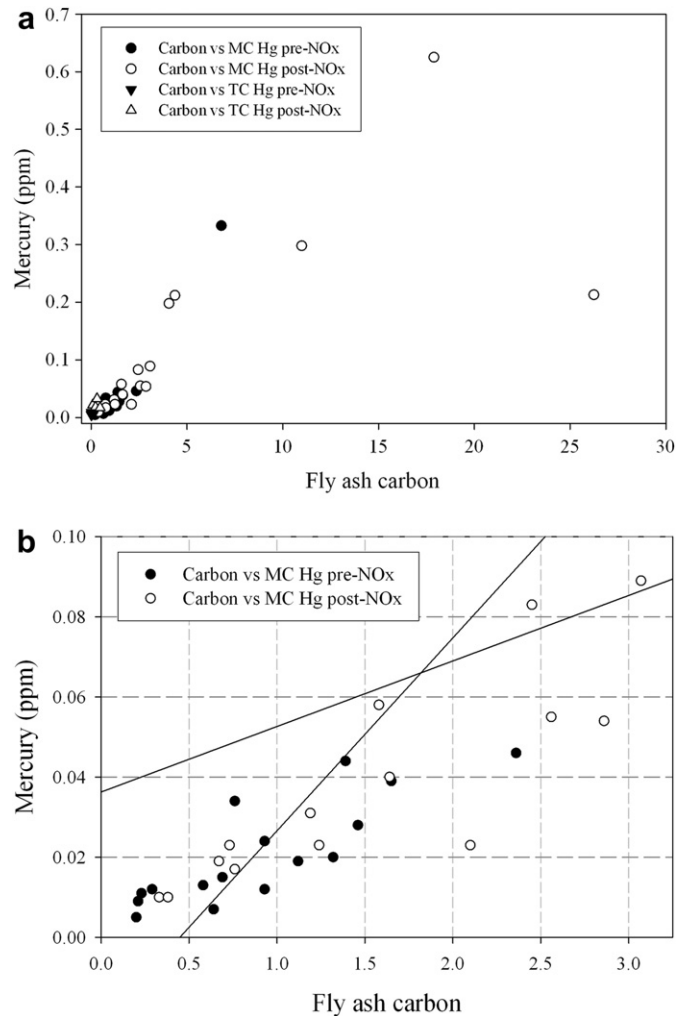

Fig. 18. a/Pre- and post-NOx-conversion Hg versus ultimate analysis carbon for two power plants (coded as MC and TC) burning Illinois Basin coal, b/Detail of low-C portion of plant MC plot. Steeper regression line is for samples with less than 5% C. Shallower regression line is for all samples, (modified after Hower et al. [19])

relationship for all first-row and second-row ESP's sampled in Kentucky in the 2002 and 2007 pentannual collections.[2] In sharp contrast to the single-ESP-row examples, the many permutations of feed-coal Hg, feed coal halogen content, flue-gas temperature, among other variables, obscure the relationship between Hg and fly ash carbon.

In contrast to the latter examples, Li et al. [79] neglected flue-gas temperature as a determining factor in the difference between the Hg content of mechanical and ESP fly ashes in the 100-MW power plant in their study, simply noting that unburned carbon was not likely to be a source of the variation in Hg between the mechanical and ESP fly ashes.

6.3. Variation in mercury capture with carbon type and feed coal rank

As noted in Section 4, there are distinct differences in carbon forms dependent upon the rank of the feed coal. This can be further

---

[2] Starting in 1992 and continuing every five years, the Center for Applied Energy Research has collected feed coal, fly ash, and other coal combustion products from each utility coal-fired power plant in Kentucky. Coincident with latter collection, a survey of ash production and utilization trends is conducted.
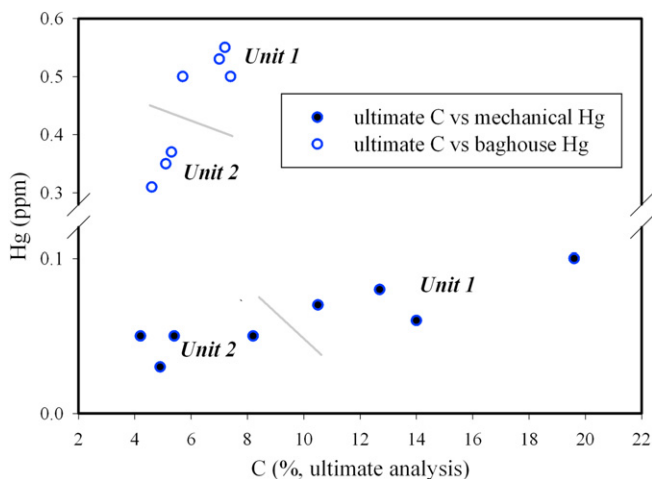
Fig. 19. Fly-ash carbon versus mercury for mechanical (cyclone) and baghouse (fabric filter) collection for two units burning high volatile A bituminous Central Appalachian coal at the same power plant, (after Hower et al. [184]).

Fig. 21. Fly-ash carbon versus mercury for a three-row electrostatic precipitator array at a Kentucky power plant burning high volatile A bituminous coal. Points represent five sample collections from 2001 to 2007. Unpublished data from University of Kentucky Center for Applied Energy Research.

complicated by the mix of coal ranks in some power plant blends; for example, the power plant in the Hower et al. [184] study now burns a Wyoming subbituminous/Colorado and Utah high volatile bituminous blend. Further, the blending of coal with non-coal carbon sources, such as tire-derived fuel and petroleum coke complicates the relationships [192–194].

Carbons from low-rank coals have proven to be highly efficient in Hg capture [67,80,195–198]. Considering fly ash Hg capture as a function of the amount of carbon in the fly ash, low-carbon Bulgarian fly ashes sourced from low-rank coals had a greater tendency to capture Hg than did bituminous-sourced Kentucky fly ashes [198]. Goodarzi and Hower [80] also demonstrated that the Alberta subbituminous-coal-derived fly ashes in their study proved to have higher Hg than the bituminous-coal-derived fly ashes. With any study comparing fly ashes from coals of different ranks, other factors, such as the chemistry of the feed coals and the engineering parameters within the respective power plants, pose complications. Indeed, Goodarzi and Hower noted that the Cl content of the feed coals was a factor in the Hg capture.
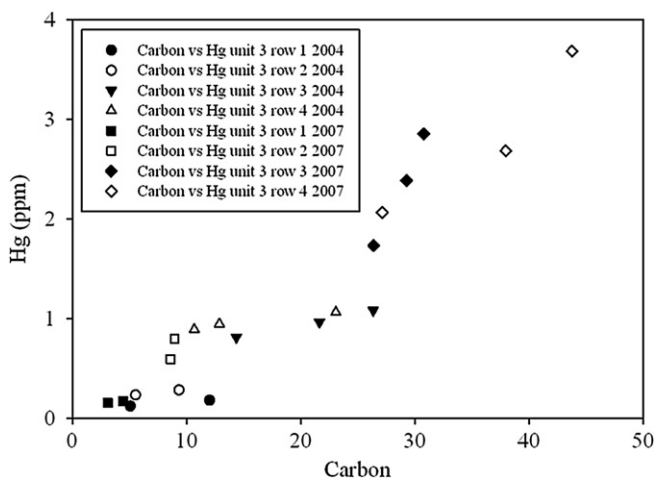

Fig. 20. Fly-ash carbon versus mercury for the first four rows of a five-row electrostatic precipitator array at a Kentucky power plant burning high volatile A bituminous coal. Points represent sample collections in 2004 and 2007. Unpublished data from University of Kentucky Center for Applied Energy Research.
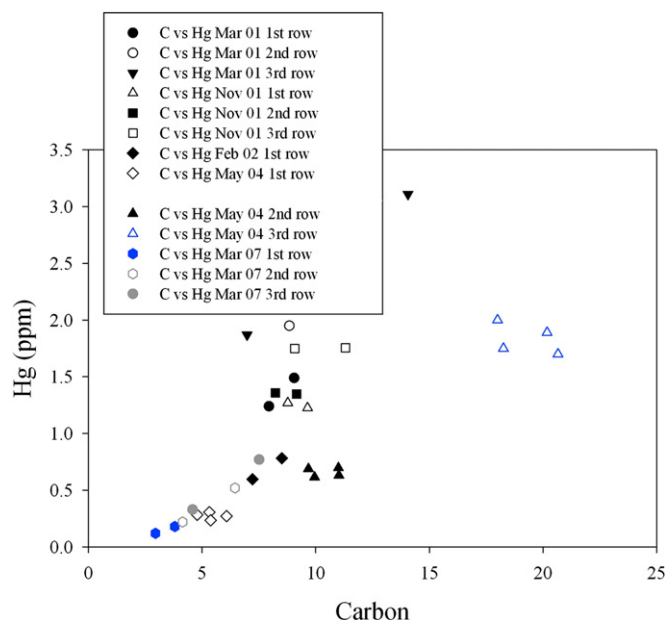
Hower et al. [72] and Maroto-Valer et al. [68,69] separated carbon from the fly ash derived from the combustion of a blend of eastern Kentucky high volatile a bituminous coals. The final step in the separation process involved the isolation of high-gradient density centrifugation splits from <1.32 to 2.15–2.30 g/cm³. While none of the splits contained pure carbon forms, the fractions dominated by anisotropic coke had a higher BET surface area and, with one exception, the highest Hg content of the fractions investigated. The exception, with the highest Hg content of all of the eight fractions analyzed, was dominated by isotropic coke. Since the samples all contained a mix of forms, the authors could not be absolutely certain that the dominant carbon form was also the dominant form with respect to Hg capture. Hill et al. [199], using fly ashes from a variety of sources, indicated that isotropic coke had a greater propensity towards Hg capture than the other fly-ash carbon forms.

Hower et al. [74] found Hg associated with Fe-rich metal inclusions, perhaps in the form of Fe spinels, within the fullerene-like carbons in the fly ash from a 220-MW power plant burning an eastern Kentucky high volatile A bituminous coal (from study by Mardon and Hower [14]). The limits of resolution of the high-resolution transmission electron microscope (HRTEM) did not allow discernment of the degree of association between the Hg and the Fe-rich metal inclusions. These results should be considered within the limited context of the coals and the resulting fly ashes in the investigation. Fly ashes derived from coals of other ranks have not yet been investigated, so we do not know if coal rank is a factor in the development of this type of carbon. In addition, we do not know the controls of coal Fe content on the development of the metal inclusions.

Suáarez-Ruiz et al. [71] and Suarez-Ruiz and Parra [70] extended the relationship between Hg and fly-ash carbon to anthracite-derived fly ashes. As with the studies of bituminous coals [68,69,72], they found a positive correlation between Hg capture with both the amount of anisotropic carbon and with the BET surface area. Lopez-Anton et al. [64] included an anthracite-derived fly ash in their investigation of fly-ash carbon petrology, BET surface
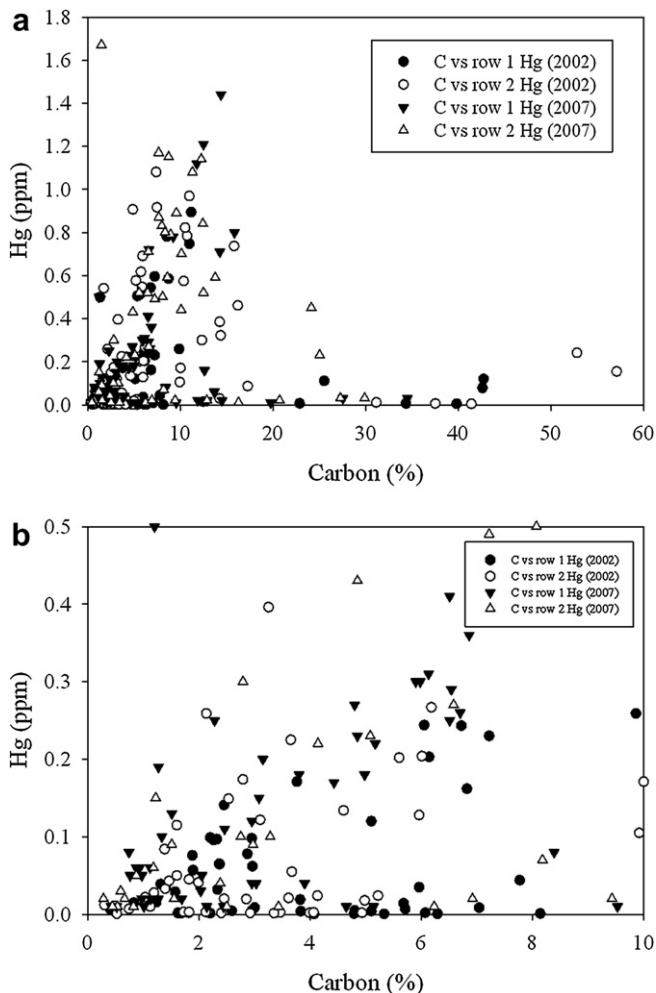
Fig. 22. a/Fly-ash carbon versus mercury for the first and second rows of electrostatic precipitators and baghouses at Kentucky power plants burning a variety of bituminous and subbituminous coals. Points represent sample collections in 2002 and 2007. Unpublished data from University of Kentucky Center for Applied Energy Research, b/Detailed view of low-C/low-Hg corner of (a).

area, and Hg capture. BET surface area per unit carbon, expressed as the loss-on-ignition, decreased from the subbituminous-derived fly ash, through the bituminous-derived fly ash, and to the anthracite-derived fly ash. Mercury retention, expressed as mg Hg/g sorbent, was highest in the bituminous-derived fly ash and lowest in the subbituminous-derived fly ash. In contrast, Kostova and Hower [198] found subbituminous-derived fly ashes to have greater affinity for Hg than Appalachian-bituminous-derived fly ashes.

7. Mechanisms of Hg capture by carbon

Various factors have been described that determine the extent of Hg capture on carbons. The importance of the acid gases in determining the reactivity of the carbon has provided valuable clues to the mechanism of Hg chemisorption and binding on carbon. Most of the mechanistic concepts were developed from studies with activated carbons, which have an isotropic nature, whereas unburned carbons represent a variety of isotropic and anisotropic forms. But the similarities in behavior of activated carbons could result from the same mechanisms operating with some of the unburned carbon [140].

Young and Musich [200] produced the seminal report on acid gas effects with Hg on a carbon surface; exposing carbons to gas-

phase Hg also containing HCl and SO$_2$. Although oxygen-containing groups on the carbon surface were suggested as being responsible for Hg sorption, no one has been able to correlate Hg capacity or reactivity with oxygen functionalities [201]. Since HCl is the exclusive form of halogen in flue gas at least at temperatures at which Hg capture occurs, we need to understand its role in the capture mechanism. Since HCl is not an oxidant, and Hg is oxidized on carbon in the absence of HCl [202], it is clear that neither HCl nor Cl$_2$ derived from HCl is responsible for oxidation of Hg on the surface. The key to understanding the role of HCl was the finding that sorption experiments conducted in low amounts of or no HCl experienced an induction effect, an initial period of time where the reactivity to Hg oxidation develops [203]. The oxidation is promoted not only by the addition of HCl, but any other acid, including small amounts of sulfuric acid [202,203]. A detailed oxidation mechanism was hypothesized to explain this acid promotion effect [203]. The mechanism involves addition of a proton or Lewis acid to a zig-zag carbon edge site to form a carbenium ion, which represents the oxidation site for the Hg or other gas components, such as SO$_2$. Later, the mechanism was somewhat modified to include the role of NO2 in helping to promote the oxidation site [204]. The combination of HCl and NO2 in the gas was a very effective promoter of Hg oxidation. The current thought is that multiple charges in the aromatic system avoids extensive delocalization and concentrates the charge and, thus, the oxidation potential at the protonated edge site [205,206].

Application of the acid promotion mechanism for Hg oxidation to the case of unburned carbon requires graphene edge structures on the carbon surface. This requirement is met for the isotropic carbons, but perhaps not as many sites are present as for an activated carbon. The requirement is more difficult to meet for an anisotropic carbon, since there will be more planar graphene carbons and fewer edge structures.

The effect of acid gases on the binding of the oxidized Hg to the carbon surface is also important to consider. Early studies elucidated the interactions of SO$_2$, NO$_2$, and moisture on oxidized Hg binding to activated carbon [141,207–209]. These publications hypothesized a competition model for Hg capture, wherein the oxidation of SO$_2$, mainly by NO$_2$, and subsequent hydrolysis on the carbon surface produced sulfuric acid. Accumulation of sulfuric acid displaces the bound Hg^{2+}, resulting in emission of mainly HgCl$_2$ from the binding sites. The extent to which this reaction occurs on unburned carbon that is collected in an ESP is unknown, but likely does contribute to the capture results under certain circumstances.

Another important point that must be considered for Hg sorption by unburned carbon is that the halogen adducts with carbon are thermodynamically stable at high temperatures. Thus, halogen (as HCl, Cl, or Cl$_2$) will react with carbon in a high temperature zone, so that the resulting promoted carbenium sites will be available for reaction with Hg when the particles have transited to lower temperature zones where the Hg is able to form stable compounds. This is different from the case where activated carbon is injected at a lower temperature, and thus lower surface areas or lower numbers of potential sites are compensated by an earlier promotion effect. Rapid Hg oxidation and capture for capture on unburned carbon may occur because the carbon does not have to wait to accumulate active sites. However, the early availability of oxidation sites also applies to SO$_2$ oxidation on the carbon surfaces. Thus, sulfuric acid forms more rapidly on the unburned carbon sites and poisoning occurs earlier, possibly explaining why attempts to demonstrate Hg capture in beds comprising materials collected from particulate control devices have not been successful.

The effects of temperature on Hg capture on carbons are generally negative, implying less capture occurs at higher temperatures. At control device temperatures, physisorption of

elemental Hg does not occur at all, but chemisorption involving formation of Hg^{2+} compounds does occur, and the temperature effect is the result of a complex set of equilibrium and kinetic factors involving the oxidized Hg species. As expected, the rate of oxidation increases with temperature [210] and, initially, the oxidized Hg is bound to the carbon. Thus, for lower capture to occur as temperature increases, the desorption rate of Hg must increase with a steeper slope, so that the net Hg captured is less at higher temperature. The bound Hg is oxidized, but the released Hg may be oxidized and/or elemental, so at least two mechanisms must be considered for desorption: 1) release of oxidized Hg via an oxidative mechanism using NO_2, and 2) release of elemental Hg via homolytic dissociation of the carbon-Hg bond [211]. Either mechanism likely occurs continuously, but relative rates are dependent on gas composition and temperature.

8. Prediction of mercury capture by carbon

Numerous studies have been published on the interpretation of data from a variety of scales ranging from bench-, pilot-, to full-scale indicating that unburned carbon (UBC) in fly ash can capture Hg in coal combustion flue gases (Section 6) [16,64,78,87,178,212]. Although not all studies are in agreement, there is a general consensus within the literature that the extent and inherent mechanism of Hg adsorption is influenced by the coal type, boiler type, temperature and quench rate, amount of UBC, surface area and porosity of UBC, surface functional groups of UBC, and flue gas composition. Several studies have directly indicated that Hg content in fly ash is directly correlated with increasing UBC content [69,87,173,178,213]. Hasset and Eylands [178] indicate that Hg capture on the inorganic components of fly ash is low compared to those of UBC, but Hower et al. [19] report that the presence of inorganic fly ash increases the complexity of the interrelationship of all of the factors that influence Hg capture.

Temperature effects influence Hg capture indirectly through UBC formation in the high temperature environment of the boiler to the quenching environment of the flue gas. Smaller particles, characteristic of those fed into a PC boiler, sinter more easily in the boiler and produce fly ash UBC particles with lower surface areas. The temperature of the boiler and residence time of the coal particles in the boiler can influence the extent of sintering further dictating the particle size and external surface area of the UBC particles produced in the fly ash. Investigations of Lu et al. [78] revealed that the Hg content of the Powder River Basin fly ashes produced from a cyclone boiler (PRB-CYC) was approximately eight times higher than Eastern Bituminous fly ashes from the PC boiler (EB-PC). However, Hower et al. [187] noted that the correlations drawn by Lu et al. [78] should be questioned based upon their small sample size of just five from cyclone boilers and four from PC boilers. Hower et al. [19] have carried out studies that indicate a wide range of fly-ash carbon contents from cyclone to PC boilers, with several of the PC fly ashes having a higher UBC content than those of the cyclone boilers. Often not discussed in detail is the change in shape that the particles undergo upon exposure to high temperature. The nonuniform temperature distribution of coal upon combustion may lead to stresses within the particles leading to the curvature associated with the graphene structures [78]. Although this particular feature has not yet been correlated to Hg capture, it could be an important aspect since it is well known that carbon nanotubes exhibit higher reactivity compared to uniform graphene sheets due to the change in the electronic structure of their active sites from their curvature.

Influencing internal surface area and porosity of UBC particles is the oxidation potential of a given particle. In general, low-rank coals are easier to activate with oxidizing gases to increase porosity versus high-rank coal [214] Another aspect to consider are low-NOx burners which are known to produce high levels of UBC (Sections 3 and 6.1). The peak flame temperature is reduced in these burners and this may influence the extent of sintering that the coal particles undergo and determine the extent to which UBC is formed in the boiler. Adsorption is an exothermic process; therefore, as flue gases are quenched it is expected that Hg adsorption will increase [77,212,215].

Fly ashes derived from lignite, subbituminous, bituminous, and anthracite have all been investigated for Hg capture, with the majority of the studies focusing on blended coals. The time–temperature profile of a coal particle in the boiler dictates the fly ash particle morphology and chemistry. In a PC boiler, approximately 70 wt. % of the coal particles are less than 75 μm and therefore burn quite easily compared to coarser particles of a cyclone boiler where approximately 100 wt. % are less than 6350 μm [216] which take a longer time to burn and form ash. A higher degree of sintering can induce the formation of graphitic carbon which has a lower surface area and number of active sites [78]. Lu et al. [78] examined fly ash from both Eastern bituminous (EB) and Powder River Basin (PRB) coal burned in PC and cyclone boilers, respectively and determined fly ashes of EB have surface areas of about 50 m^2/g while those of PRB are about 150 m^2/g. Kiilatos et al. [67] reported surface areas for UBC of bituminous-derived fly ash of between 20 and 80 m^2/g and of subbituminous-derived fly ash between 230 and −400 m^2/g. Lopez-Anton et al. [64] found that, in contrast to elemental Hg, oxidized Hg capture correlated with surface area. However, with elevated levels of Hg (0.4 μg/mL), a synthetic gas mixture to simulate the flue gas environment, and a sorbent temperature of 120 °C, their [64] studies did not take place in a realistic coal combustion flue gas environment. Even the effects of temperature on Hg capture on carbons are generally negative, that is less capture occurs at higher temperatures (Section 6.2). The sorption is entirely chemisorption at control device temperatures, and the rate of oxidation increases with temperature [210]. Thus, the reason for lower capture at higher temperatures must be that the desorption rate of Hg is higher at the higher temperature. The UBC particles are at least an order of magnitude lower in surface area than the typical commercially available activated carbons, e.g., Norit Americas activated carbon for Hg removal has a surface area of 600 m^2/g [217] and Calgon HGR has a surface area of 1000 m^2/g.

Serre and Silcox [75] carried out a series of Hg adsorption experiments by passing Hg^0 diluted by N_2 through both fixed- and fluidized-bed reactors containing various fly ash and activated carbon samples. As with Lopez-Anton et al.'s [64] investigations, the experiments took place with Hg levels an order of magnitude higher than typically found in coal combustion flue gases and at a fixed temperature of 121 °C. They found that the level of Hg^0 adsorbed was directly proportional to the carbon content within each of the fly ashes tested. Additionally, Serre and Silcox [75] tested Calgon HGR and found that it adsorbed twice the amount of Hg as any of the fly ashes investigated. The fly ashes with the highest surface area tested was derived from the Clark and Huntington power plants. The coal source was not specified, but the each fly ash type had surface areas of 65.1 and 63.8 m^2/g, respectively. The adsorption ability of a given fly ash particle can be associated with its BET surface area which increases from inertinite, isotropic coke, to anisotropic coke [72]. However, many of the fly ash adsorption studies carried out fail to discuss the coal from which the fly ash was derived. Future studies would benefit from deeper discussions regarding the source of the fly ash and its related formation pathway which is likely related Hg capture potential. Depending upon the type of coal combusted, UBC particles with varying morphologies and surface characteristics may result and drive the Hg adsorption and oxidation reactions.

An understanding of the chemical nature of the UBC within the fly ash is crucial to determining the mechanism by which elemental and oxidized forms of Hg are adsorbed. Lopez-Anton et al. [64] determined the characteristics of a variety of fly ash samples taken from the combustion of feed coal blends and have related these characteristics to Hg^0 and HgCk retention. Three of the four samples they investigated were from a pulverized coal combustion power plant with the fourth sample from a fluidized-bed plant. The fuel burned in these different power plants includes (1) varying blends from a mixture of high-rank coals (CTA), (2) bituminous coals (CTSR), (3) subbituminous coals (CTES) (CTA, CTSR, CTES, and CTP, below, are codes used by the authors [64]). The fly ash taken from the fluidized-bed plant where a blend of bituminous and coal wastes were mixed with limestone was termed CTP. Lopez-Anton et al. [64] provide detailed characterization of each of these fly ashes examined including anisotropic, isotropic, and inorganic components in addition to BET surface area and LOI. Highlights are presented here to provide an indication of the primary UBC components potentially responsible for Hg retention.

The CTA fly ash examined came from burning high-rank coals, that is, mainly anthracites with smaller quantities of semi-anthracites and bituminous coals. It was found that the unburned carbon in the fly ash was primarily anisotropic, unfused, and dense particles derived from anthracitic vitrinite. The fused, porous, and vesiculated materials reported are derived from burning inertinite. The CTA fly ash was mainly found to be comprised of inorganic glassy material such as alumino silicates (65–70 vol. %). The CTSR fly ash was derived from burning bituminous coal and is similar to CTA with the exception that the anisotropic carbons are primarily fused, porous and vesiculated structures. CTES fly ash were formed when burning low-rank coal such as subbituminous or lignite. The UBC particles comprised within this fly ash type were reported to be mainly isotropic fused and porous structures, formed from vitrinite macerals present in the low-rank coal. In terms of their inorganic counterparts, CTES fly ash was comprised of alumino silicates in addition to quartz. Comprised mainly of undifferentiated anisotropic fragments, the CTP fly ash investigated by Lopez et al. [64] was found to be very different compared to the others from pulverized-coal-fired boilers. Additionally, a higher fraction of oxides were found in the CTP fly ash compared to the others.

Within this study it was found that the most favorable fly ash for Hg^0 capture was the bituminous-derived CTSR, having the greatest number of anisotropic fused structures. Their study corroborated previous findings of Suarez-Ruiz et al. [71] and Suarez-Ruiz and Parra [70] in that no relationship was found between the total isotropic composition, total amount of mineral matter, and Hg retention. Lopez-Anton et al. [64] noted that $HgCl_2$ follows a similar trend to Hg^0 in that it was captured mostly in the fly ash containing anisotropic components. Hassett and Eylands [178] found Hg adsorbed to fly ash containing inertinite and coked carbon. Lu et al. [64] investigated oxidation reactivity of Powder River Basin subbituminous-cyclone and Eastern US bituminous-pulverized-coal fly ashes motivated by the parallel relationship between the number of active sites available for oxidation by forming C–O groups and the same sites being available for potential Hg adsorption. They related the surface area with the internal pore area and number of active sites and found these to affect the oxidation rate of UBC in a similar manner to Hg adsorption. The surface area of the PRB-CYC fly ashes was three times higher than that of EB-PC in addition to a higher oxidation activity. The amount of Hg adsorbed in the PRB-CYC ashes was about an order of magnitude higher than the EB-PC ashes.

Although lower-rank coals are more easily activated by oxidizing gases and, hence, have higher internal surface areas which can potentially play a dominant role in capturing Hg, other aspects of coal's chemistry such as Cl content can also play a major role (see also Section 5). High levels of particulate-bound Hg are correlated with coals, primarily bituminous, containing Cl levels > 200–300 Cl µg/g (dry basis) [77]. Oxygen functional groups play a role in Hg adsorption by serving as both oxidation catalysts and binding sites [201,218]. The primary Hg species observed on activated carbon surfaces is not elemental but oxidized Hg, implying that Hg is bound to the surface by an oxidizing functional group such as oxygen or a halogen (see Section 7). Studies supporting the oxidized nature of Hg on the carbon surface are based upon X-ray absorption fine structure spectroscopy [219] and desorption [207,208].

Low-rank coals, such as lignite, tend to have higher concentrations of Ca, promoting Hg oxidation [220]. This is supported by Gale et al.'s [221] experimental search aimed at characterizing the majority of full-scale U.S. coal-fired plants, isolating each factor that could potentially influence Hg capture. They found the greatest influences on Hg capture to be unburned carbon content, Cl concentrations, and also a synergistic enhancement of Hg by carbon and Ca in fly ash. Gale et al. [221] proposed that the presence of Ca enhances the amount of HgCl found on the UBC surface and in the absence of Ca, Hg^0 adsorbs onto chlorinated-carbon sites and desorbs as oxidized Hg, resulting in minimal Hg capture.

9. Conclusions

- The most fundamental control on Hg in the fly ash carbons is the amount of Hg in the feed coal. Mercury in coal is most commonly in sulfide minerals, but can occur in a number of other minerals, as well as in organic association. In association with pyrite, Hg concentration can vary across several orders of magnitude.
- Aside from the amount of Hg in the feed coal to the power plant, the controls on Hg in fly ash are:
  (1) The temperature at the ash collection hopper, the lower the temperature, the greater the chance of Hg adsorption;
  (2) The amount of carbon in the fly ash, the higher the carbon, the greater the chance of Hg adsorption;
  (3) The rank of the feed coal and the consequent type of carbon, with low-rank-coal-derived carbons having a greater Hg-capture tendency than bituminous-coal-derived carbons and, with the series of bituminous-derived carbons, adsorption and BET surface area increasing in the order inertinite to isotropic coke to anisotropic coke; and
  (4) The overall chemistry of the feed coal, which determines the components of the flue gas, with fly ash carbons from high-Cl coals having a greater tendency to adsorb Hg.
- The potential of unburned carbon in fly ash to contribute to Hg capture is a function of the amount (noted above), the size distribution, surface area, and surface chemistry. All of these are a complex function of conditions in the boiler, which, in turn, can be impacted by factors such as the conversion to low-NOx combustion or the fineness of the coal feed, among many other factors.
- Mercury is in the gaseous elemental form in the boiler. Even though thermodynamic equilibrium suggests that, at the temperature of the inlet to the APCD, the mercury will oxidize to HgCk, this step is kinetically limited in coal-fired boilers. A small fraction of the Hg will be homogeneously oxidized under these conditions; however, Hg will also be oxidized heterogeneously with the fly ash. This oxidized Hg has the potential to be absorbed onto fly ash carbons, given the favorable temperature in the APCD.Acid gases, including HCl and H_2SO_4, in the flue gas can enhance the oxidation of Hg. The

combination of HCl and NO_2 in the gas is an effective promoter of Hg oxidation.

- Halogen adducts with carbon are thermodynamically stable at high temperatures, therefore, halogen (as HCl, Cl, or Cl_2) will react with carbon in a high temperature zone. The resulting promoted carbenium sites will be available for reaction with Hg at lower temperature zones where the Hg is able to form stable compounds.
- The presence of Ca, found more frequently in low-rank coals than in bituminous coals, can enhance Hg oxidation.

10. Future research challenges

- The current extent of HRTEM-STEM-EELS studies of the nature of the very-fine fly-ash carbon and the associated metal inclusions is limited to high volatile bituminous, medium-S coals. Logical extensions of this work would be to higher and lower coal ranks, as well as to a wider mix of sulfur contents.
- While it is clear that the organic portion of the fly ash influences mercury reactivity, future work should include further studies of inorganic FA.
- Recent field work has shown the impact of SO_3 on performance of activated carbon for mercury removal. SO_3 probably also contributes to lower amounts of mercury sorption by unburned carbon in ash, although this is less well documented. Initial fundamental work on behavior of activated carbon in the presence of SO_3 should be expanded to include unburned carbon.

Acknowledgements

References

[1] United States Environmental Protection Agency. Electric utility steam generating units section 112 rule making, http://www.epa.gov/ttn/atw/combust/utiltox/utoxpg.html; 2007 [accessed 7.07.09].
[2] Quick JC, Brill TC, Tabet DE. Mercury in US coal: observations using the COALQUAL and ICR data. Environmental Geology 2003;43(3):247–59.
[3] United States Environmental Protection Agency. Clean air interstate rule, http://www.epa.gov/CAIR/; 2005a [accessed 7.07.09].
[4] United States Environmental Protection Agency. Clean air mercury rule, http://www.epa.gov/camr/; 2005b [accessed 7.07.09].
[5] United States Court of Appeals District of Columbia Circuit. State of North Carolina, Petitioner v. Environmental Protection Agency, respondent, http://pacer.cadc.uscourts.gov/common/opinions/200807/05-1244-1127017.pdf; 2008a [accessed 7.07.09].
[6] United States Court of Appeals District of Columbia Circuit, State of New Jersey, et al. Petitioner v. environmental protection agency, respondent, http://pacer.cadc.uscourts.gov/docs/common/opinions/200802/05-1097a.pdf; 2008b [accessed 7.07.09].
[7] New York Times. Clean slate on clean air, http://www.nvtimes.com/2009/03/08/opinion/08sun2.html; 2009 [accessed 8.03.09].
[8] Bravender R. Bush rules on toxic mercury from power plants overturned. Scientific American, http://www.sciam.com/article.cfm?id=toxic-mercury-rule-over; 2009 [accessed 7.07.09].
[9] United States Environmental Protection Agency. United States Court of Appeals for the District of Columbia Circuit, decided December 23, 2008, No. 05–1244 state of North Carolina, Petitioner V. Environmental Protection Agency, respondent, utility air regulatory group, et al., Intervenors. http://www.epa.gov/airmarkets/progsregs/cair/docs/CAIRRemandOrder.pdf, 2009, [accessed 7.07.09].
[10] Milford JB, Pienciak A. After the clean air mercury rule: prospects for reducing mercury emissions from coal-fired power plants. Environmental Science and Technology 2009;43(8):2669–73.
[11] Nelson S, Landreth R, Liu X, et al. Power-plant mercury control results with brominated PAC and ESPs. In: Presented at the air quality V conference, September 19–21, 2005, Arlington, VA.
[12] Toole-O'Neil B, Tewalt SJ, Finkelman RB, Akers DJ. Mercury concentration in coal – unraveling the puzzle. Fuel 1999;78(1):47–54.
[13] Goodarzi F, Goodarzi NN. Mercury in western Canadian subbituminous coal – a weighted average study to evaluate potential mercury reduction by selective mining. International Journal of Coal Geology 2004;58(4):251–9.
[14] Mardon SM, Hower JC. Impact of coal properties on coal combustion by-product quality: examples from a Kentucky power plant. International Journal of Coal Geology 2004;59(3–4):153–69.
[15] Mastalerz M, Hower JC, Drobniak A, Mardon SM, Lis G. From in-situ coal to fly ash: a study of coal mines and power plants from Indiana. International Journal of Coal Geology 2004;59(3–4):171–92.
[16] Sakulpitakphon T, Hower JC, Trimble AS, Schram WH, Thomas GA. Mercury capture by fly ash: study of the combustion of a high-mercury coal at a utility boiler. Energy and Fuels 2000;14(3):727–33.
[17] Sakulpitakphon T, Hower JC, Schram WH, Ward CR. Tracking mercury from the mine to the power plant: geochemistry of the Manchester coal bed, Clay county, Kentucky. International Journal of Coal Geology 2004;57(2):127–41.
[18] Finkelman RB. Modes of occurrence of potentially hazardous elements in coal: levels of confidence. Fuel Processing Technology 1994;39(1–3):21–34.
[19] Hower JC, Robl TL, Anderson C, Thomas GA, Sakulpitakphon T, Mardon SM, et al. Characteristics of coal combustion products (CCP's) from Kentucky power plants, with emphasis on mercury content. Fuel 2005;84(11):1338–50.
[20] Hower JC. Maceral/microlithotype partitioning with particle size of pulverized coal: examples from power plants burning central Appalachian and Illinois basin coals. International Journal of Coal Geology 2008;73(3–4):213–8.
[21] Hower JC, Eble CF, Quick JC. Mercury in eastern Kentucky coals: geologic aspects and possible reduction strategies. International Journal of Coal Geology 2005;62(4):223–36.
[22] Hower JC, Mastalerz M, Drobniak A, Quick JC, Eble CF, Zimmerer MJ. Mercury content of the Springfield coal, Indiana and kentucky. International Journal of Coal Geology 2005;63(3–4):205–27.
[23] Diehl SF, Goldhaber MB, Hatch JR. Modes of occurrence of mercury and other trace elements in coals from the warrior field, black warrior basin, northwestern Alabama. International Journal of Coal Geology 2004;59(3–4):193–208.
[24] Ding Z, Zheng B, Long J, Belkin HE, Finkelman RB, Chen C, et al. Geological and geochemical characteristics of high arsenic coals from endemic arsenosis areas in southwestern Guizhou province, China. Applied Geochemistry 2001;16(11–12):1353–60.
[25] Feng X, Hong Y. Modes of occurrence of mercury in coals from Guizhou, People's Republic of China. Fuel 1999;78(10):1181–8.
[26] Zhang J, Ren D, Zheng C, Zeng R, Chou C-, Liu J. Trace element abundances in major minerals of late Permian coals from southwestern Guizhou province, China. International Journal of Coal Geology 2002;53(l):55–64.
[27] Zhang J, Ren D, Zhu Y, Chou C-, Zeng R, Zheng B. Mineral matter and potentially hazardous trace elements in coals from Qianxi fault depression area in southwestern Guizhou, China. International Journal of Coal Geology 2004;57(1):49–61.
[28] Hower JC, Campbell JL, Teesdale WJ, Nejedly Z, Robertson JD. Scanning proton microprobe analysis of mercury and other trace elements in Fe-sulfides from a Kentucky coal. International Journal of Coal Geology 2008;75(2):88–92.
[29] Seredin VV. The au-PGE mineralization at the Pavlovsk brown coal deposit, Primorye. Geology of Ore Deposits 2004;46(l):36–63.
[30] Seredin VV, Finkelman RB. Metalliferous coals: a review of the main genetic and geochemical types. International Journal of Coal Geology 2008;76(4):253–89.
[31] Hower JC, Robertson JD. Clausthalite in coal. International Journal of Coal Geology 2003;53(4):219–25.
[32] Dai S, Zeng R, Sun Y. Enrichment of arsenic, antimony, mercury, and thallium in a late Permian anthracite from Xingren, Guizhou, southwest China. International Journal of Coal Geology 2006;66(3):217–26.
[33]. Piedad-Sanchez N, Izart A, Martinez L, Suarez-Ruiz I, Elie M, Menetrier C. Paleothermicity in the central Austrian coal basin, north Spain. International Journal of Coal Geology 2004;58(4):205–29.
[34] Dai S, Ren D, Chou C-, Li S, Jiang Y. Mineralogy and geochemistry of the No. 6 coal (Pennsylvanian) in the Junger coalfield, Ordos basin, China. International Journal of Coal Geology 2006;66(4):253–70.
[35] Brownfield ME, Affolter RH, Cathcart JD, Johnson SY, Brownfield IK, Rice CA. Geologic setting and characterization of coals and the modes of occurrence of selected elements from the Franklin coal zone, Puget group, John Henry No. 1

mine, King County, Washington, USA. International Journal of Coal Geology 2005;63(3–4):247–75.

[36] Yudovich YE, Ketris MP. Mercury in coal: a review, part 1. Geochemistry. International Journal of Coal Geology 2005;62(3):107–34.

[37] Helmuth R. Fly ash in cement and concrete. Portland Cement Association; 1987.

[38] Hachman L, Burnett A, Gao Y, Hurt R, Suuberg E. Surfactant adsorptivity of carbon solids from pulverized coal combustion under controlled conditions. In: Twenty-seventh symposium (international) on combustion, 2965–2971. Pittsburgh: The Combustion Institute; 1998.

[39] Freeman E, Gao YM, Hurt RH, Suuberg EM. Interactions of carbon-containing fly ash with commercial air-entraining admixtures for concrete. Fuel 1997;74(8):761–5.

[40] Gao Y-, Shim H-, Hurt RH, Suuberg EM, Yang NYC. Effects of carbon on air entrainment in fly ash concrete: the role of soot and carbon black. Energy and Fuels 1997;11(2):457–62.

[41] Pedersen KH, Jensen AD, Berg M, Olsen LH, Dam-Johansen K. The effect of combustion conditions in a full-scale low-NOx coal fired unit on fly ash properties for its application in concrete mixtures. Fuel Processing Technology 2009;90(2):180–5.

[42] Beer JM. Combustion technology developments in power generation in response to environmental challenges. Progress in Energy and Combustion Science 2000;26:301–27.

[43] Veranth JM, Fletcher TH, Pershing DW, Sarofim AF. Measurement of soot and char in pulverized coal fly ash. Fuel 2000;79(9):1067–75.

[44] Fletcher TH, Ma J, Rigby JR, Brown AL, Webb BW. Soot in coal combustion systems. Progress in Energy and Combustion Science 1997;23(3):283–301.

[45] Stephens DL, McFadden T, Heath OD, Mauldin RF. The effect of sonication on the recovery of polycyclic aromatic hydrocarbons from coal stack ash surfaces. Chemosphere 1994;28(10):1741–7.

[46] Liu K, Xie W, Zhao ZB, Pan WP, Riley JT. Investigation of polycyclic aromatic hydrocarbons in fly ash from fluidized bed combustion systems. Environmental Science and Technology 2000;34:2273–9.

[47] Wornat MJ, Guran S, Cheng H, Marsh ND. Compositional analysis of organic extracts from fly ash samples of coal-burning utilities. In: ACS division of fuel chemistry preprints, Fall Annual Meeting, 1998.

[48] Burgess RM, Perron MM, Friedman CL, Suuberg EM, Pennell KG, Cantwell MG, et al. Evaluation of the effects of coal fly ash amendments on the toxicity of a contaminated marine sediment. Environmental Toxicology and Chemistry 2009;28(1):26–35.

[49] Hsu T-. Adsorption of an acid dye onto coal fly ash. Fuel 2008;87(13–14):3040–5.

[50] Gao Y, Chen X, Fujisaki G, Mehta A, Suuberg E, Hurt R. Dry and semi-dry methods for removal of ammonia from pulverized fuel combustion fly ash. Energy and Fuels 2002;16(6):1398–404.

[51] Lee CW, Serre SD, Zhao Y, Sung JL, Hastings TW. Mercury oxidation promoted by a selective catalytic reduction catalyst under simulated powder river basin coal combustion conditions. Journal of the Air and Waste Management Association 2008;58(4):484–93.

[52] Wang J, Wang T, Mallhi H, Liu Y, Ban H, Ladwig K. The role of ammonia on mercury leaching from coal fly ash. Chemosphere 2007;69(10):1586–92.

[53] Turner JR, Choné S, Duduković MP. Ammonia/fly ash interactions and their impact on flue gas treatment technologies. Chemical Engineering Science 1994;49(24 PART A):4315–25.

[54] Kulaots I, Gao YM, Hurt RH, Suuberg EM. Adsorption of ammonia on coal fly ash. In: Proc. 2001 International Ash Utilization Symposium, Paper #59. University of Kentucky, http://www.flvash.info; 2001.

[55] Hurt RH, Gibbins JR. Residual carbon from pulverized coal fired boilers: 1. Size distribution and combustion reactivity. Fuel 1995;75(4):471–80.

[56] Hurt RH, Davis KA, Yang NYC, Headley TJ, Mitchell GD. Residual carbon from pulverized coal fired boilers: 2. Morphology and physicochemical properties. Fuel 1995;75(9):1297–306.

[57] Davis KA, Hurt RH, Yang NYC, Headley TJ. Evolution of char chemistry, crystallinity, and ultrafine structure during pulverized-coal combustion. Combustion and Flame 1995;100(1–2):31–40.

[58] Gao YM, Kulaots I, Chen X, Suuberg EM, Hurt RH, Veranth JM. The effect of solid fuel type and combustion conditions on residual carbon properties and fly ash quality. Proceedings of the Combustion Institute 2002;29:475–83.

[59] Sharonova OM, Anshits NN, Yumashev VV, Anshits AG. Composition and morphology of char particles of fly ashes from industrial burning of high-ash coals with different reactivity. Fuel 2008;87(10–11):1989–97.

[60] Shibaoka M. Carbon content of fly-ash and size distribution of unburnt char particles in fly-ash. Fuel 1986;65(3):449–50.

[61] Shibaoka M. Microscopic investigation of unburnt char in fly-ash. Fuel 1986;64(2):263–9.

[62] Bailey JG, Tate A, Diessel CFK, Wall TF. A char morphology system with applications to coal combustion. Fuel 1990;69(2):225–39.

[63] Lopez-Anton MA, Diaz-Somoano M, Martinez-Tarzona MR. Retention of elemental mercury in fly ashes in different atmospheres. Energy and Fuels 2007;21(1):99–103.

[64] Lopez-Anton MA, Abad-Valle P, Diaz-Somoano M, Suarez-Ruiz I, Martinez-Tarzona MR. The influence of carbon particle type in fly ashes on mercury adsorption. Fuel 2009;88:1194–200.

[65] Baltrus JP, Wells AW, Fauth DJ, Diehl JR, White CM. Characterization of carbon concentrates from coal-combustion fly ash. Energy and Fuels 2001;15(2):455–62.

[66] Kulaots I, Aarna I, Callejo M, Hurt RH, Suuberg EM. Development of porosity during coal char combustion. Proceedings of the Combustion Institute 2002;29:495–501.

[67] Kulaots I, Hurt RH, Suuberg EM. Size distribution of unburned carbon in coal fly ash and its implications. Fuel 2004;83(2):223–30.

[68] Maroto-Valer M, Taulbee DN, Hower JC. Novel separation of the differing forms of unburned carbon present in fly ash using density gradient centrifugation. Energy and Fuels 1999;13(4):947–53.

[69] Maroto-Valer M, Taulbee DN, Hower JC. Characterization of differing forms of unburned carbon present in fly ash separated by density gradient centrifugation. Fuel 2001;80:795–800.

[70] Suarez-Ruiz I, Parra JB. Relationship between textural properties, fly ash carbons, and Hg capture in fly ashes derived from the combustion of anthracitic pulverized feed blends. Energy and Fuels 2007;21(4):1915–23.

[71] Suarez-Ruiz I, Hower JC, Thomas GA. Hg and Se capture and fly ash carbons from combustion of complex pulverized feed blends mainly of anthracitic coal rank in spanish power plants. Energy and Fuels 2007;21(1):59–70.

[72] Hower JC, Mercedes Maroto-Valer M, Taulbee DN, Sakulpitakphon T. Mercury capture by distinct fly ash carbon forms. Energy and Fuels 2000;14(1):224–6.

[73] Hower JC, Robl TL, Thomas GA, Hopps SD, Grider M. Chemistry of coal and coal combustion products from Kentucky power plants: Results from the 2007 sampling, with emphasis on selenium. Coal Combustion & Gasification Products 2009;1. doi:10.4177/CCGP-D-09-00013.1.

[74] Hower JC, Graham UM, Dozier A, Tseng MT, Khatri RA. Association of the sites of heavy metals with nanoscale carbon in a Kentucky electrostatic precipitator fly ash. Environmental Science and Technology 2008;42(22):8471–7.

[75] Serre SD, Silcox GD. Adsorption of elemental mercury on the residual carbon in coal fly ash. Industrial and Engineering Chemistry Research 2000;39(6):1723–30.

[76] Ikeda M, Makino H, Morinaga H, Higashiyama K, Kozai Y. Emission characteristics of NOx and unburned carbon in fly ash during combustion of blends of bituminous/sub-bituminous coals. Fuel 2003;82:1851–7.

[77] Senior CL, Johnson SA. Impact of carbon-in-ash on mercury removal across particulate control devices in coal-fired power plants. Energy and Fuels 2005;19:859–63.

[78] Lu Y, Rostam-Abadi M, Chang R, Richardson C, Paradis J. Characteristics of fly ashes from full-scale coal-fired power plants and their relationship to mercury adsorption. Energy and Fuels 2007;21(4):2112–20.

[79] Li S, Cheng C-M, Chen B, Cao Y, Vervynckt J, Adebambo A, et al. Investigation of the relationship between particulate-bound mercury and properties of fly ash in a full-scale 100 MWe pulverized coal combustion boiler. Energy and Fuels 2007;21(6):3292–9.

[80] Goodarzi F, Hower JC. Classification of carbon in Canadian fly ashes and their implications in the capture of mercury. Fuel 2008;87(10–11):1949–57.

[81] Yu JL, Lucas JA, Wall TF. Formation of the structure of chars during devolatilization of pulverized coal and its thermoproperties: a review. Progress in Energy and Combustion Science 2007;33(2):135–70.

[82] Senneca O. Burning and physico-chemical characteristics of carbon in ash from a coal fired power plant. Fuel 2008;87:1207–16.

[83] Bartonova L, Klika Z, Spears DA. Characterization of unburned carbon from ash after bituminous coal and lignite combustion in CFBs. Fuel 2007;86:455–63.

[84] Jimenez S, Ballester J. Study of the evolution of particle size distributions and its effects on the oxidation of pulverized coal. Combustion and Flame 2007;151:482–94.

[85] Hurt RH. Structure, properties and reactivity of solid fuels. Proceedings of the Combustion Institute 1998;27:2887–904.

[86] Butz J, Smith J. Coal fly ash as a sorbent for mercury. Research Summary. ADA Technologies, Inc.; November 9, 1999.

[87] Pavlish JH, Sondreal EA, Benson SA, et al. Status review of mercury control options for coal-fired power plants. Fuel Processing Technology 2003;82:89–165.

[88] Essenhigh RH. Fundamentals of coal combustion [Chapter 19] of. In: Elliott MA, editor. The chemistry of coal utilization, Second Supplementary Volume. Wiley; 1981.

[89] Smoot LD. Coal and char combustion [Chapter 10] in. In: Bartok W, Sarofim AF, editors. Fossil fuel combustion. Wiley and Sons; 1991.

[90] Walker Jr PL, Rusinko Jr F, Austin LG. Gsaa reactions of carbon. In: Eley D, et al., editors. Advances in catalysis, vol. XI. New York: Academic Press; 1959. p. 133.

[91] Beeley T, Crelling J, Gibbins J, Hurt RH, Lunden M, Man C, et al. Transient high-temperature thermal deactivation of monomaceral-rich coal chars. Proceedings of the Combustion Institute 1996;26:3103–10.

[92] Eaton AM, Smoot LD, Hill SC, Eatough CN. Components, formulations, solutions, evaluation and application of comprehensive combustion models. Progress in Energy and Combustion Science 1999;25(4):387–436.

[93] Williams A, Backreedy R, Habib R, Jones JM, Pourkashanian M. Modeling coal combustion: the current position. Fuel 2002;81:605–18.

[94] Pallares J, Arauzo I, Williams A. Integration of CFD codes and advanced combustion models for quantitative burnout determination. Fuel 2007;86:2283–90.

[95] Stopford PJ. Recent applications of CFD modelling in the power generation and combustion industries. Applied Mathematical Modelling 2002;26:351–74.

[96] Hurt R, Sun J-, Lunden M. A kinetic model of carbon burnout in pulverized coal combustion. Combustion and Flame 1998;113(1–2):181–97.

[97] Sun J, Hurt RH, Niksa S, Muzio L, Mehta A, Stallings J. A simple numerical model to estimate the effect of coal selection on pulverized fuel burnout. Combustion Science and Technology 2003;175(6):1085–108.

[98] Stephenson P. Computer modeling of the combined effects of plant conditions and coal quality on burnout in utility furnaces. Fuel 2007;86:2026–31.

[99] Cloke M, Wu T, Barranco R, Lester E. Char characterisation and its application in a coal burnout model. Fuel 2003;82:1989–2000.

[100] Wu T, Lester E, Cloke M. A burnout prediction model based around char morphology. Energy and Fuels 2006;20:1175–83.

[101] Pallares J, Arauzo I, Diez LI. Numerical prediction of unburned carbon levels in large pulverized coal utility boilers. Fuel 2005;84:2364–71.

[102] Pallares J, Arauzo I, Teruel E. Development of and engineering system for unburned carbon prediction. Fuel 2009;88:187–94.

[103] Gera D, Mathur M, Freeman M, O'Dowd W. Moisture and char reactivity modeling in pulverized coal combustors. Combustion Science and Technology 2001;172:35–69.

[104] Mitchell RE, Ma L, Kim B. On the burning behavior of pulverized coal chars. Combustion and Flame 2007;151:426–36.

[105] Gavalas GR. A random capillary model with application to char gasification at chemically controlled rates. AIChE Journal 1980;26:577–85.

[106] Bhatia SK, Perlmutter DD. A random pore model for fluid-solid reactions 1. Isothermal, kinetic control. AIChE Journal 1980;26:379–86.

[107] Oh MS, Peters WA, Howard JB. An experimental and modeling study of softening coal pyrolysis. AIChE Journal 1989;35(5):775–92.

[108] Yu JL, Strezov V, Lucas J, Liu GS, Wall TF. A mechanistic study on char structure evolution during coal devolatilization-experiments and model predictions. Proceedings of the Combustion Institute 2002;29:467–73.

[109] Yamashita T, Fujii Y, Morozumi Y, Aoki H, Miura T. Modeling of gasification and fragmentation behavior of char particles having complicated structures. Combustion and Flame 2006;146:85–94.

[110] Nandi BN, Brown TD, Lee GK. Inert coal macerals in combustion. Fuel 1977;56(2):125–30.

[111] Vleeskens JM, Menendez RM, Roos CM, Thomas CG. Combustion in the burnout stage: the fate of inertinite. Fuel Processing Technology 1993;36(1–3):91–9.

[112] Lester E, Cloke M, Allen M. Char characterization using image analysis techniques. Energy and Fuels 1996;10(3):696–703.

[113] Vassilev SV, Menendez R, Borrego AG, Diaz-Somoano M, Martinez-Tarazona MR. Phase-mineral and chemical composition of coal fly ashes as a basis for their multicomponent utilization. 3. Characterization of magnetic and char concentrates. Fuel 2004;83(11–12):1563–83.

[114] Vassilev SV, Vassileva CG, Karayigit AI, Bulut Y, Alastuey A, Querol X. Phase-mineral and chemical composition of composite samples from feed coals, bottom ashes and fly ashes at the Soma power station, Turkey. International Journal of Coal Geology 2005;61(1–2):35–63.

[115] Vassilev SV, Vassileva CG, Karayigit AI, Bulut Y, Alastuey A, Querol X. Phase-mineral and chemical composition of fractions separated from composite fly ashes at the Soma power station, Turkey. International Journal of Coal Geology 2005;61(1–2):65–85.

[116] Gray RJ, Devanney KF. Coke carbon forms: microscopic classification and industrial applications. International Journal of Coal Geology 1986;6(3):277–97.

[117] Hower JC, Rathbone RF, Graham UM, Groppo JG, Brooks SM, Robl TL, Medina SS. Approaches to the petrographic characterization of fly ash. In: 11th international coal testing conference; 1995. pp. 49–54.

[118] Hower JC, Suarez-Ruiz I, Mastalerz M. An approach toward a combined scheme for the petrographic classification of fly ash: Revision and clarification. Energy and Fuels 2005;19(2):653–5.

[119] Hower JC, Mastalerz M. An approach toward a combined scheme for the petrographic classification of fly ash. Energy and Fuels 2001;15(5):1319–21.

[120] Alvarez D, Borrego AG, Menendez R. Unbiased methods for the morphological description of char structures. Fuel 1997;76(13):1241–8.

[121] International Committee for Coal and Organic Petrology. The new vitrinite classification (ICCP system 1994): international committee for coal and organic petrology (ICCP). Fuel 1998;77(5):349–58.

[122] International Committee for Coal and Organic Petrology. New inertinite classification (ICCP system 1994). Fuel 2001;80(4):459–71.

[123] Sýkorová I, Pickel W, Christanis K, Wolf M, Taylor GH, Flores D. Classification of huminite – ICCP system 1994. International Journal of Coal Geology 2005;62(1–2):85–106.

[124] Shim H-, Sarofim A, Davis K, Bockelie M. Modeling of the impact of low-NOx combustion systems. Clearwater Coal Conference; 2003.

[125] Linak WP, Yoo J-I, Wasson SJ, Zhu W, Wendt JOL, Huggins FE, et al. Ultrafine ash aerosols from coal combustion: characterization and health effects. Proceedings of the Combustion Institute; 2007:311929–37.

[126] Chen Y, Shah N, Huggins FE, Huffman GP, Dozier A. Characterization of ultrafine coal fly ash particles by energy-filtered TEM. Journal of Microscopy 2005;217(3):225–34.

[127] Chen Y, Shah N, Huggins FE, Huffman GP. Transmission electron microscopy investigation of ultrafine coal fly ash particles. Environmental Science and Technology 2005;39(4):1144–51.

[128] Frandsen F, Dam-Johansen K, Rasmussen P. Trace elements from combustion and gasification of coal – an equilibrium approach. Progress in Energy and Combustion Science 1994;20(2):115–38.

[129] Linak WP, Wendt JOL. Trace metal transformation mechanisms during coal combustion. Fuel Processing Technology 1994;39(1–3):173–98.

[130] Senior CL, Sarofim AF, Zeng T, Helble JJ, Mamani-Paco R. Gas-phase transformations of mercury in coal-fired power plants. Fuel Processing Technology 2000;63(2):197–213.

[131] Edwards JR, Srivastava RK, Kilgroe JD. A study of gas-phase mercury speciation using detailed chemical kinetics. Journal of the Air and Waste Management Association 2001;51(6):869–77.

[132] Fujiwara N, Moritomi H, Tuji T, Yamada, M. A study of mercury transformation behavior on coal combustion. In: International conference on air quality II: mercury, trace elements, and paniculate matter. McLean, VA; 19–21 September 2000.

[133] Niksa S, Helble JJ, Fujiwara N. Kinetic modeling of homogeneous mercury/oxidation: the importance of NO and H2O in predicting oxidation in coal-derived systems. Environmental Science and Technology 2001;35(18):3701–6.

[134] Qiu J, Sterling RO, Helble JJ. Development of an improved model for determining the effects of SO2 on homogeneous mercury oxidation. In: 28th international technical conference on coal utilization & fuel systems, clearwater, FL; 10–13 March 2003.

[135] Sliger RN, Kramlich JC, Marinov NM. Towards the development of a chemical kinetic model for the homogeneous oxidation of mercury by chlorine species. Fuel Processing Technology 2000;65:423–38.

[136] Senior C, Sadler B, Sarofim A. Modeling mercury behavior in practical combustion systems. San Diego, CA: American Chemical Society; 13–17 March 2005.

[137] Widmer NC, West J, Cole JA. Thermochemical study of mercury oxidation in utility boiler flue gases. In: Air & waste management association 93rd annual conference and exhibition. Proceedings. Salt Lake City, UT; 18–22 June 2000.

[138] Lee CW, Kilgroe JD, Ghorish SB. Speciation of mercury in the presence of coal and waste combustion fly ashes. In: Air & waste management association 93rd annual conference and exhibition. Proceedings. Salt Lake City, UT; 18–22 June 2000.

[139] Niksa S, Fujiwara N, Fujita Y, Tomura K, Moritomi H, Tuji T, et al. A mechanism for mercury oxidation in coal-derived exhausts. Journal of the Air and Waste Management Association 2002;52(8):894–901.

[140] Olson ES, Laumb JD, Benson SA, Dunham GE, Sharma RK, Mibeck BA, et al. An improved model for flue gas-mercury interactions on activated carbon. In: DOE-EPRI-U.S. EPA-A&WMA combined power plant air pollutant control symposium – the mega symposium, proceedings. Washington, DC; 19–22 May 2003.

[141] Olson ES, Crocker CR, Benson SA, Pavlish JH, Holmes MJ. Surface compositions of carbon sorbents exposed to simulated low-rank coal flue gases. Journal of the Air and Waste Management Association 2005;55(6):747–54.

[142] Senior CL. Oxidation of mercury across selective catalytic reduction catalysts in coal-fired power plants. Journal of the Air and Waste Management Association 2006;56(1):23–31.

[143] US Department of Energy National Energy Technology Laboratory. Coal power plant database, http://www.netl.doe.gov/energy-analyses/technology.html; 2007 [accessed 29.05.09].

[144] Afonso RF, Senior CL., Assessment of mercury emissions from full scale power plants. In: EPRI-EPA-DOE-AWMA mega symposium and mercury conference. Chicago, IL; 21–23 August 2001.

[145] Kilgroe JD, Sedman CB, Srivastava RK, Ryan JV, Lee CW, Thorneloe SA. Control of mercury emissions from coal-fired electric utility boilers. Interim Report; EPA-600/R-01–109. National Risk Management Laboratory; April 2002.

[146] Senior C. Review of the role of aqueous chemistry in mercury removal by acid gas scrubbers on incinerator systems. Environmental Engineering Science 2007;24(8):1129–34.

[147] Laudal D. Effect of selective catalytic reduction on mercury. 2002 field studies Update. Palo Alto, CA: EPRI; 2002. Product ID 1005558.

[148] Chu P, Laudal D, Brickett L, Lee CW. Power plant evaluation of the effect of SCR technology on mercury. In: DOE-EPRI-U.S. EPA-A&WMA combined power plant air pollutant control symposium – the mega symposium. Washington, DC; 19–22 May 2003.

[149] Lee CW, Srivastava RK, Ghorishi SB, Hastings TW, Stevens FM. Study of speciation of mercury under simulated SCR NOx emission control conditions. In: DOE-EPRI-U.S. EPA-A&WMA combined power plant air pollutant control symposium – the mega symposium. Washington, DC; 19–22 May 2003.

[150] Withum JA. Evaluation of mercury emissions from coal-fired facilities with SCR and FGD systems; Final Report. In: US Department of Energy National Energy Technology Laboratory Cooperative Agreement DE-FC26–02NT41589; April, 2006.

[151] Canadian Electricity Association (CEA). Mercury program, sampling and analysis, participant data (preliminary) 2004. http://www.ceamercuryprogram.ca/EN/sampling_data.html [accessed 2.06.09].

[152] Sjostrom S, Bustard CJ, Durham M, Chang R. Mercury removal trends in full-scale ESPs and fabric filters. In: EPRI-EPA-DOE-AWMA mega symposium and mercury conference. Chicago, IL; 21–23 August 2001.

[153] Meij R. Trace element behavior in coal-fired power plants. Fuel Processing Technology 1994;39(1–3):199–217.

[154] Smith RD, Campbell JA, Felix WD. Atmospheric trace element pollutants from coal combustion. Mining Engineering 1980;32(ll):1603–13.

[155] Querol X, Fernandez-Turiel J, Lopez-Soler A. Trace elements in coal and their behaviour during combustion in a large power station. Fuel 1995;74(3):331–43.

[156] Martinez-Tarazona MR, Spears DA. The fate of trace elements and bulk minerals in pulverized coal combustion in a power station. Fuel Processing Technology 1996;47(1):79–92.

[157] Vassilev SV, Vassileva CG. Geochemistry of coals, coal ashes and combustion wastes from coal-fired power stations. Fuel Processing Technology 1997;51(1–2):19–45.

[158] Yan R, Lu X, Zeng H. Trace elements in Chinese coals and their partitioning during coal combustion. Combustion Science and Technology 1999;145(1):57–81.

[159] Senior CL, Bool III LE, Morency JR. Laboratory study of trace element vaporization from combustion of pulverized coal. Fuel Processing Technology 2000;63(2):109–24.

[160] Senior CL, Helble JJ, Sarofim AF. Emissions of mercury, trace elements, and fine particles from stationary combustion sources. Fuel Processing Technology 2000;65:263–88.

[161] Ward CR. Analysis and significance of mineral matter in coal seams. International Journal of Coal Geology 2002;50(1–4):135–68.

[162] Sloss LL. Trace elements – controlling emissions from coal combustion. International Journal of Environment and Pollution 2002;17(1–2):110–25.

[163] Pires M, Querol X. Characterization of Candiota (south Brazil) coal and combustion by-product. International Journal of Coal Geology 2004;60(1):57–72.

[164] Levandowski J, Kalkreuth W. Chemical and petrographical characterization of feed coal, fly ash and bottom ash from the Figueira power plant, Parana, Brazil. International Journal of Coal Geology 2009;77(3–4):269–81.

[165] Meij R, te Winkel BH. Trace elements in world steam coal and their behaviour in Dutch coal-fired power stations: a review. International Journal of Coal Geology 2009;77(3–4):289–93.

[166] Depoi FS, Pozebon D, Kalkreuth WD. Chemical characterization of feed coals and combustion-by-products from Brazilian power plants. International Journal of Coal Geology 2008;76(3):227–36.

[167] Mardon SM, Hower JC, O'Keefe JMK, Marks MN, Hedges DH. Coal combustion by-product quality at two stoker boilers: coal source vs. fly ash collection system design. International Journal of Coal Geology 2008;75(4):248–54.

[168] Goodarzi F, Huggins FE, Sanei H. Assessment of elements, speciation of As, Cr, Ni and emitted Hg for a Canadian power plant burning bituminous coal. International Journal of Coal Geology 2008;74(1):1–12.

[169] Bool III LE, Helble JJ. A laboratory study of the partitioning of trace elements during pulverized coal combustion. Energy and Fuels 1995;9(5):880–7.

[170] Robl TL, Hower JC, Groppo JG, Graham UM, Rathbone RF, Taulbee DN, et al. The impact of conversion to low-NOx burners on ash characteristics. In: Proc. 1995 Int. joint power generation conference; vol. 1; 1995. pp. 469–76.

[171] Hower JC, Graham UM, Wong AS, Robertson JD, Haeberlin BO, Thomas GA, et al. Influence of flue-gas desulfurization systems on coal combustion byproduct quality at Kentucky power stations burning high-sulfur coal. Waste Management 1998;17(8):523–33.

[172] Hower JC, Thomas GA, Palmer J. Impact of the conversion to low-NOx combustion on ash characteristics in a utility boiler burning western US coal. Fuel Processing Technology 1999;61(3):175–95.

[173] Hower JC, Thomas GA, Trimble AS. Impact of conversion to low-NOx combustion on fly ash quality: investigation of a unit burning high-sulfur coal. In: International ash utilization symposium;1999.

[174] Hower JC, Trimble AS, Eble CF, Palmer CA, Kolker A. Characterization of fly ash from low-sulfur and high-sulfur coal sources: partitioning of carbon and trace elements with particle size. Energy Sources 1999;21(6):511–25.

[175] Otero-Rey JR, Lopez-Vilarino JM, Moreda-Pineiro J, Alonso-Rodriguez E, Muniategui-Lorenzo S, Lopez-Mahia P, et al. As, Hg, and Se flue gas sampling in a coal-fired power plant and their fate during coal combustion. Environmental Science and Technology 2003;37(22):5262–7.

[176] Lindau L. Mercury sorption to coal fly ash. Staub, Reinhaltung Der Luft 1983;43(4):166–7.

[177] Sen AK, De AK. Adsorption of mercury (II) by coal fly ash. Water Research 1987;21(8):885–8.

[178] Hassett DJ, Eylands KE. Mercury capture on coal combustion fly ash. Fuel 1999;78(2):243–8.

[179] Gibb WH, Clarke F, Mehta AK. Fate of coal mercury during combustion. Fuel Processing Technology 2000;65:365–77.

[180] Meij R, Vredenbregt LHJ, Te Winkel H. The fate and behavior of mercury in coal-fired power plants. Journal of the Air and Waste Management Association 2002;52(8):912–7.

[181] Sloss LL. Mercury – emissions and controls; International Energy Agency CCC 58 2002.

[182] Tan Y, Mortazavi R, Dureau B, Douglas MA. An investigation of mercury distribution and speciation during coal combustion. Fuel 2004;83(16):2229–36.

[183] Li J, Gao X, Goeckner B, Kollakowsky D, Ramme B. A pilot study of mercury liberation and capture from coal-fired power plant fly ash. Journal of the Air and Waste Management Association 2005;55(3):258–64.

[184] Hower JC, Finkelman RB, Rathbone RF, Goodman J. Intra- and inter-unit variation in fly ash petrography and mercury adsorption: examples from a western Kentucky power station. Energy and Fuels 2000;14(1):212–6.

[185] Sakulpitakphon T, Hower JC, Trimble AS, Schram WH, Thomas GA. Arsenic and mercury partitioning in fly ash at a Kentucky power plant. Energy and Fuels 2003;17(4):1028–33.

[186] Hower JC, Sakulpitakphon T, Trimble AS, Thomas GA, Schram WH. Major and minor element distribution in fly ash from a coal-fired utility boiler in Kentucky. Energy Sources, Part A: Recovery, Utilization and Environmental Effects 2006;28(1):79–95.

[187] Hower JC, Valentim B, Kostova IJ, Henke KR. Discussion on "Characteristics of fly ashes from full-scale coal-fired power plants and their relationship to mercury adsorption" by Lu et al. Energy and Fuels 2008;22(2):1055–8.

[188] Valentim B, Hower JC, Flores D, Guedes A. Notes on the efficacy of wet versus dry screening of fly ash. Minerals and Metallurgical Processing 2008;25:143–8.

[189] Hower JC, Rathbone RF, Robl TL, Thomas GA, Haeberlin BO, Trimble AS. Case study of the conversion of tangential- and wall-fired units to low-NO(x) combustion: impact on fly ash quality. Waste Management 1998;17(4):219–29.

[190] Hower JC, Robl TL, Rathbone RF, Schram WH, Thomas GA. Characterization of pre- and post-NOx conversion fly ash From the Tennessee Valley Authority's John Sevier fossil plant. In: Proceedings, 12th International Symposium on Coal Combustion By-product (CCB) Management and Use; January 26–30, 1997. Orlando, FL, Published by Electric Power Research Institute, EPRITR-107055-V2. pp. 39-1–39-13.

[191] Robl T, Groppo JG, Brooks S, Hower JC, Medina SS. Case studies of low NOx burner retrofit: I. the affect of loss on ignition, particle size and chemistry of the fly ash. In: Proceedings, 11th international symposium on use and management of coal combustion byproducts; 1995.

[192] Hower JC, Robertson JD, Elswick ER, Roberts JM, Brandsteder K, Trimble AS, et al. Further investigation of the impact of the co-combustion of tire-derived fuel and petroleum coke on the petrology and chemistry of coal combustion products. Energy Sources, Part A: Recovery, Utilization and Environmental Effects 2007;29(5):439–61.

[193] Hower JC, Thomas GA, Mardon SM, Trimble AS. Impact of co-combustion of petroleum coke and coal on fly ash quality: case study of a western Kentucky power plant. Applied Geochemistry 2005;20(7):1309–19.

[194] Hower JC, Robertson JD, Roberts JM. Petrology and minor element chemistry of combustion by-products from the co-combustion of coal, tire-derived fuel, and petroleum coke at a western Kentucky cyclone-fired unit. Fuel Processing Technology 2001;74(2):125–42.

[195] Goodarzi F, Reyes J, Abrahams K. Comparison of calculated mercury emissions from three Alberta power plants over a 33 week period - influence of geological environment. Fuel 2008;87(6):915–24.

[196] Goodarzi F. Characteristics and composition of fly ash from Canadian coal-fired power plants. Fuel 2006;85(10–11):1418–27.

[197] Goodarzi F. Petrology of subbituminous feed coal as a guide to the capture of mercury by fly ash - influence of depositional environment. International Journal of Coal Geology 2005;61(1–2):1–12.

[198] Hower JC, Kostova IJ. Comparative studies of mercury capture by Bulgarian and Kentucky fly ash carbons. Annual Meeting. New Orleans: American Chemical Society; 6–9 April 2008.

[199] Hill RL, Sarkar SL, Rathbone RF, Hower JC. An examination of fly ash carbon and its interactions with air entraining agent. Cement and Concrete Research 1997;27(2):193–204.

[200] Young BC, Musich MA. Screening of carbon-based sorbents for the removal of elemental mercury from simulated combustion flue gas. Preprint Papers – American Chemical Society, Division of Fuel Chemistry 1995;40(4):833–7.

[201] Ghorishi SB, Keeney RM, Serre SD, Gullet BK, Jozewicz WS. Development of a Cl-impregnated activated carbon for entrained-flow capture of elemental mercury. Environmental Science and Technology 2002;36:4454–9.

[202] Olson ES, Miller SJ, Sharma RK, Dunham GE, Benson SA. Catalytic effects of carbon sorbents for mercury capture. Journal of Hazardous Materials 2000;74:61–79.

[203] Olson ES, Mibeck BA, Benson SA, Laumb JD, Crocker CR, Dunham GE, et al. The mechanistic model for flue gas-mercury interactions on activated carbons: the oxidation site. Preprint Papers – American Chemical Society, Division of Fuel Chemistry 2004;49:6.

[204] Olson ES, Mibeck BA, Dunham GE, Miller SJ, Pavlish JH. Control of flue gas mercury emissions: effects of acid gases on sorbent reactivity. Preprint Papers – American Chemical Society, Division of Fuel Chemistry 2009;54(1):236–8.

[205] Azenkeng A, Laumb JD, Jensen RR, Olson ES, Benson SA, Hoffmann MR. Carbene proton attachment energies: theoretical study. Journal of Physical Chemistry A 2008;112:5269–77.

[206] Olson ES, Azenkeng A, Laumb J, Jensen R, Benson S. New developments in the theory and modeling of mercury oxidation and binding on activated carbons in flue gas. In: Proceedings, Air Quality VI; 2007.

[207] Carey TR, Hargrove OW, Richardson CF, Chang R, Meserole FR. Factors affecting mercury control in utility flue gas using activated carbon. Journal of the Air and Waste Management Association 1998;48:1166–74.

[208] Miller SJ, Dunham GE, Olson ES, Brown TD. Flue gas effects on a carbon-based mercury sorbent. Fuel Processing Technology 2000;65-66:343–63.

[209] Laumb JD, Benson SA, Olson ES. X-ray photoelectron spectroscopy analysis of mercury sorbent surface chemistry. Fuel Processing Technology 2004;85(6–7):577–85.

[210] Olson ES, Mibeck BA. Oxidation kinetics of mercury in flue gas. Preprint Papers – American Chemical Society, Division of Fuel Chemistry 2005;50(1):68–70.

[211] Olson ES, Sharma RK. The stability of mercury (ii) compounds in process gas streams. Preprint Papers – American Chemical Society, Division of Fuel Chemistry 2002;42(1):759.

[212] Dunham GE, DeWall RA, Senior CL. Fixed-bed studies of the interactions between mercury and coal combustion fly ash. Fuel Processing Technology 2003;82:197–213.

[213] Gullett BK, Ghorishi B, Jozewicz W, Ho K. The advantage of Illinois coal for FGD removal of mercury. Technical Report. Carterville, IL: Illinois Clean Coal Institute; October 31, 2001.

[214] Suuburg EM, Aarna KI, Callejo M, Hsu A. A study of activation of coal char, Final Technical Progress Report, DE-FG2699FT40582; 2003.

[215] Karatza D, Lancia A, Musmarra D, Pepe F. Adsorption of metallic mercury on activated carbon. In: Twenty-sixth symposium (international) on combustion. Pittsburgh: The Combustion Institute; 1996. p. 2439–45.

[216] United States Environmental Protection Agency (U.S. EPA). Compilation of air pollutant emission factors. In: Stationary point and area sources. 5th ed., vol. 1; Jan. 1995, http://wwww.epa.gov/ttn/chief/ap42/ch01/index.html; Jan. 1995.

[217] Bustard J, Durham M, Starns T, Lindsey C, Martin C, Schlager R, et al. Full-scale evaluation of sorbent injection for mercury control on coal-fired power plants. Fuel Processing Technology 2004;85:549–62.

[218] Chen X, Mehta A, Paradis J, Hurt RH. Developing ash-utilization-friendly sorbents for gas-phase mercury removal in coal combustion flue gas. In: Proceedings of the 29th International Technical Conference on Coal Utilization and Fuel Systems. Gaithersburg, MD: Coal Technology Association; 2004.

[219] Huggins FE, Yap N, Huffman GPXAFS. Investigation of mercury sorption on carbon-based and other sorbent materials. Japanese Journal of Applied Physics 1999;38:588–91.

[220] Niksa S, Fujiwara N. Predicting extents of mercury oxidation in coal-derived flue gases. Journal of the Air and Waste Management Association 2005;55:930–9.

[221] Gale TK, Lani BW, Offen GR. Mechanisms governing the fate of mercury in coal-fired power systems. Fuel Processing Technology 2008;89(2):139–51.